Potential Anti-Fibrotic Effects of Interleukin-10 on Fibroblasts

Bachelor Project Sophie Zomers
S4903889
8 April 2024
Supervisor: Prof. Dr. Klaas Poelstra
Department: Nanomedicine & Drug Targeting (NDT)

Content

Abstract

Many studies are searching for therapies against liver fibrosis. This disease involves all sorts of processes like inflammation and the accumulation of collagen, Understanding the mechanisms behind the development of fibrosis will give new insights into the drug development. Interleukin-10 (IL-10) has attracted interest as it is thought that this cytokine potentially has anti-fibrotic effects. This study analyzed the anti-fibrotic and inflammatory effects of IL-10 on NIH-3T3 cells. The nitric oxide production (NO assay) was measured after stimulation with different cytokines like PDGF-β, TGF-β, IFN-γ and IL-10. Inflammation was induced by LPS. IFN-γ showed pro-inflammatory effects on the production of NO. IL-10 showed varying results and was unable to induce inflammation. Furthermore, the DHPAA-assay was used to measure the collagen concentration after stimulation with TGF-β and LPS. Using a digestion time of 20 hours let to a higher collagen concentration than a digestion time of 1 hour. However, no effects of TGF-β were visible. Lastly, qPCR was used to measure the gene expression of HAS1, HAS2 and HAS3, genes encoding for hyaluronic synthase. One of the components of the extracellular matrix is hyaluronic acid, synthesized by hyaluronic synthase. Fibrosis is characterized by less hyaluronic acid and it is therefore thought that the gene expression of HAS would also be lower. The 3T3 cells were stimulated with TGF-β, IFN-γ, IL-10 and LPS. IFN-γ with LPS showed an increase in HAS gene expression. This gene expression was lower with the addition of IL-10. In summary, interleukin-10 showed anti-inflammatory effects on the expression of HAS1, 2 and 3. However, no anti-fibrotic effects had been observed.

Introduction

Liver fibrosis is a chronic liver disease. It is characterised by the proliferation of fibroblasts, deposition of fibrous connective tissue and the infiltration of inflammatory cells. The liver has a complex architecture and many functions. The Glisson's capsule encapsulates the liver and is composed of connective tissue. Within this capsule, the liver is split into lobules. These are composed of numerous hexagonal shaped functional units with a characteristic arrangement. The major parenchymal cells in the liver are hepatocytes. These cells play a major role in the biochemical and metabolic functions of the liver. [1]
Viral infections like hepatitis B (HBV) and C (HCV), but also fatty diets, alcohol abuse, non-alcoholic fatty liver disease (NAFLD) and autoimmune diseases are responsible for damaging the hepatocytes and thereby cause liver fibrosis. [2] This includes scar tissue formation and loss of liver function. If the inflammation is permanent, it will lead to cirrhosis over time. Cirrhosis is an end-stage fibrotic complication where there is extensive scarring, leading to even more loss of function. This will cause liver failure and eventually, organ transplantation is the last resource. [3]

Normally, quiescent hepatic stellate cells (HSCs) are present in the liver where they metabolize vitamin A and produce the collagen rich extracellular matrix. The cells can be found in the space of Disse and they are able to secrete matrix metalloproteinases (MMPs), such as MMP-1. These are degradative enzymes, promoting the degradation of extracellular matrix (ECM). Additionally, HSCs produce tissue inhibitors of matrix metalloproteinases (TIMPs), like TIMP-1. TIMP-1 can prevent the ECM degradation by blocking MMP and thereby prevent HSC apoptosis. This interaction is highly regulated. By this, the body sustains injury and the organs repair themselves by collagen deposition, also called fibrogenesis. [4]

The response to injury starts in the cells. Damaged hepatocytes, liver endothelial cells and macrophages (Kupffer cells) release pro-inflammatory signals, such as transforming growth factor-beta (TGF-b), platelet-derived growth factor (PDGF), reactive oxygen species (ROS) and damage-associated molecular patterns (DAMPs). By this, HSCs are activated and change their phenotype from the quiescent state to a myofibroblast-like phenotype. This is the beginning of all sorts of processes: cell proliferation and survival, increase in cell contractability, chemotaxis, leukocyte recruitment and more cytokine and growth factor release. However, the most important function of myofibroblasts is the formation of scar tissue. [5]
Myofibroblasts are able to synthesize and secrete ECM proteins, especially collagen I and III, which are collagen fibers. These give structural support, leading to more rigid and stiff scar tissue. Besides, the activation of HSC also leads to the upregulation of TIMP-1 and downregulation of MMPs. As less cells are degraded and more produced, the ECM proteins are accumulating and cause scar tissue formation. [6] Due to the many processes, several cell types work together and there is extensive crosstalk between them. Eventually, the persistent proliferation of HSCs and inflammation in the liver will lead to the accumulation of ECM proteins and thereby liver fibrosis. [7] An overview of the main interactions between cell types and cytokines during the whole process is shown in Figure 1.

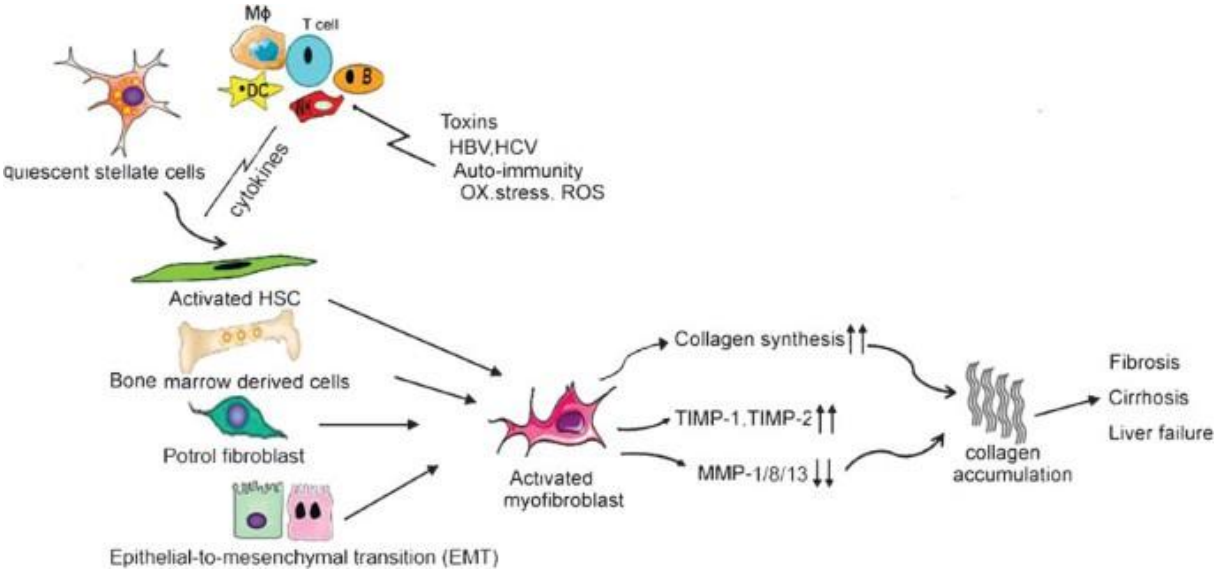

Figure 1: The pathway leading to liver fibrosis. Different cytokines are released by the activation of immune cells by injury. The cytokines activate quiescent stellate cells, leading to activated myofibroblasts. Collagen synthesis and TIMP-1 and TIMP-1 expression is upregulated. MMP expression is downregulated. This leads to collagen accumulation and eventually liver fibrosis. [8]

Lipopolysaccharide (LPS) is one of the main inducers of an acute inflammatory response in the cells. This endotoxin can be found in the outer membrane of gram-negative bacteria and starts inflammation by stimulating the release of various inflammatory cytokines in different cell types. As liver fibrosis is characterized by chronic inflammation, the effect of inflammation on fibroblasts can be tested by using LPS as a stimulus. [9] It is thought that LPS stimulates the Toll Like Receptor 4 (TLR4) pathway in fibroblasts. This pathway is involved in the expression of collagen. Therefore, the addition of LPS to fibroblasts should induce inflammation, like nitric oxide (NO) release, and it should induce the formation of hypertrophic scars and thereby collagen synthesis. [10]
NO is considered to be a pro-inflammatory mediator. Therefore, by measuring the NO produced by the cells, the amount of inflammation can be determined. This principle can be used to determine the effect of different stimuli on fibroblasts. [11, 12] One of these stimulations can be interleukin-10 (IL-10)

Interleukin-10 is considered to be an anti-inflammatory cytokine produced by many immune cells like macrophages, B cells, granulocytes, dendritic cells and many more. It has an immunosuppressive effect by being a potent negative feedback regulator, effecting the control and resolution of inflammation. There are two main pathways by which inflammatory responses are limited. First, IL-10 inhibits the antigen presentation of dendritic cells. Secondly, macrophage activation and infiltration is inhibited. Consequently, pro-inflammatory cytokine release is reduced. [13] However, in recent studies IL-10 has been found to be both pro- and anti-fibrotic, depending on the cell type. It is found that it is anti-fibrotic in HSC, but pro-fibrotic in macrophages. [6] Thus, the exact role of IL-10 in fibrosis remains unclear. That is why people also looked for other cytokines that show anti-fibrotic effects, such as interferon gamma (IFN-γ).

Interferon gamma (IFN-γ) is a pro-inflammatory cytokine which is involved in the modulation and induction of immune responses. [14] It is able to stimulate different cell types, like macrophages, T cells and fibroblasts. With this, it increases phagocytosis and the intracellular

killing of pathogens. [15, 16]. Among the few, interferon-gamma is also able to exert anti-fibrotic effects by inhibiting collagen expression and the development of myofibroblasts. [17]
In a previous study it was found that interferon-γ can enhance NO release by fibroblasts when stimulated with LPS. [12] Therefore, IFN-γ is used to study the effect of IL-10 on the inflammatory response of fibroblasts, the main producers of collagens.

Collagens are proteins composed of three alpha chains and they contain at least one triple-helical domain. They are components of the ECM and thereby contribute to the structure and mechanical properties of tissue. As said before, the collagen production is dysregulated in the case of fibrosis and the tissue becomes more rigid and stiff. Due to the importance of collagen, it could be a potential measurement of fibrosis. [18] One of the most fundamental components of ECM is hyaluronan, also called hyaluronic acid (HA).
HA is a ubiquitously expressed glycosaminoglycan that provides strength and flexibility to tissues. [19] Due to its negative charge and hydrophilicity it is able to retain water in the matrix. Therefore, it provides a hydrated space around the cells and gives elasticity to the ECM. Liver fibrosis is characterised by a lower amount of HA in between the collagen fibres and thereby a more rigid and stiff ECM. The acid is synthesized by hyaluronan synthases (HAS). [20, 21]
This enzyme has three different isotopes with the following genes: HAS1, HAS2, HAS3. There are notable differences in the chain length of their end product. [22, 23] Full-length HA enhances pro-resolving functions, whereas HA fragments stimulate macrophages for a pro-inflammatory response. [24] Thus, high molecular weight HA is beneficial in the case of liver fibrosis. Besides, there are differences in enzymatic kinetics as HAS1 and HAS2 have a faster elongation rate. Due to the importance of hyaluronic acid in the ECM, the genes are important biomarkers for liver fibrosis.

This study has the aim of finding an anti-fibrotic effect of IL-10 on stimulated fibroblasts. Different aspects of liver fibrosis will be studied, including the production of NO, the collagen concentration and HAS gene expression with quantitative PCR.

Materials and Methods

Reagents

The following stimulants were used: murine PDGF-BB (CAT: 315-18-10UG), murine IFN-γ (CAT: 315-05-100UG), human IL-10 (CAT: 200-10), murine IL-10 (CAT: 210-10-10UG), human TGF-β1 (CAT: 100-21C-10UG), lipopolysaccharides from Escherichia coli (CAT: L2880-100MG). Furthermore, Collagen Type I Rat Tail (4,24 mg/mL stock, CORNING 354236) was used for the standard curve of the DHPAA-assay. During the assay, collagenase from Clostridium histolyticum (CAS No: 9001-12-1) and 3, 4-dihydroxyphenylacetic acid (DHPAA)(CAS No: 102-32-9) were used.

Cell culture

The NIH-3T3 fibroblasts were cultured in Dulbecco's Modified Eagle's Medium (DMEM) with 10% Fetal Bovine Serum. The cells were incubated at 37 degrees with 5% CO_2 in a T-25 flask. The cells were grown till 80-90% confluence and then harvested with trypsin (TEP) for further growth and experiments. The complete protocol can be found in **Appendix A**.

Nitric Oxide assay

The detailed protocol performed for the NO assay is stated in **Appendix B.**

Experiment 1: Nitric oxide estimation in NIH-3T3 cells with PDGF-β, INF-γ and LPS

The timeline for this experiment is shown in **Figure 2** The NIH-3T3 cells were seeded in a 12-well plate at a density of $2 \cdot 10^4$ cells/cm^2. Medium was added and the cells were incubated for 24h. Next, the medium was removed and new medium was added. 1,2 mL medium was added to each well instead of 1 mL. This was done to retain sufficient medium for the cells after the removal of 250 µL for the NO assay samples. Four wells were stimulated with PDGF-β (40 ng/mL) and four were stimulated with INF-γ (40 ng/mL). The cells were incubated for 3h. Subsequently, LPS (100 ng/mL) was added to 6 wells and the cells were incubated for 24h.
After the incubation time, 250 µL samples were taken from the medium and stored at -18 °C. The cells were incubated for 48h. Again, 250 µL samples were taken from the medium and an NO assay was performed.

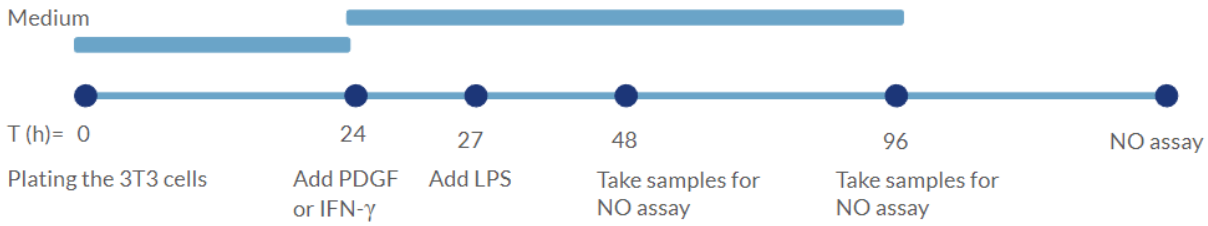

Figure 2: Timeline of NO assay experiment 1, including the stimulation and the time by which the medium is used.

Experiment 2: Nitric oxide estimation in NIH-3T3 cells with IFN-γ, IL-10 and LPS

The timeline for this experiment is shown in **Figure 3**. The NIH-3T3 cells were seeded in a 12-well plate at a density of $3 \cdot 10^3$ cells/cm^2. Medium was added and the cells were incubated for 24h. Next, the medium was removed and 1 mL new medium was added containing the different stimulants. Each stimulant was added to two wells. The cells were treated with solely medium, IFN-γ (40 ng/mL), human IL-10 (30 ng/mL) and IFN-γ and human IL-10. The cells were incubated for 3h. After this, LPS (100 ng/mL) was added to half of the wells, including IFN-γ, IL-10 and IFN-γ

and IL-10. The cells were incubated for 72h. After the incubation time, 250 µL samples were taken from the medium and an NO assay was performed.

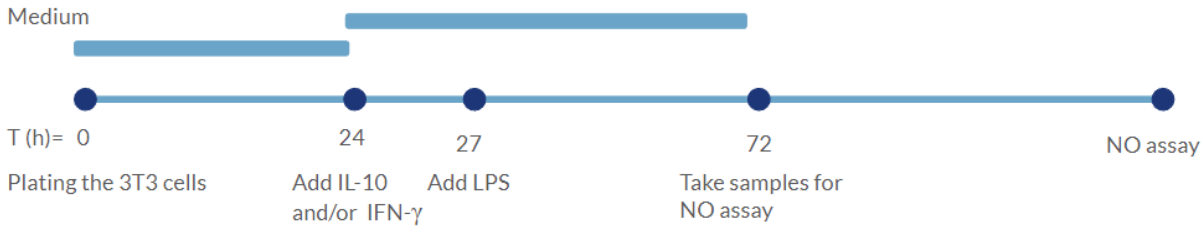

Figure 3: Timeline of NO assay experiment 2 and 3, including the stimulation and the time by which the medium is used.

Experiment 3: Nitric oxide estimation in NIH-3T3 cells with IFN-γ, IL-10 and LPS
The timeline for this experiment is shown in **Figure 3.** Almost the same protocol has been used as in experiment 2. However, there is a difference in the used densities. In experiment 3, the cells were seeded with a density of $2 \cdot 10^4$ cells/cm^2 and stimulated with IFN-γ, human IL-10, IFN-γ and human IL-10 with the same concentrations as used before. Additionally, two wells were seeded with a density of $3 \cdot 10^3$ cells/cm^2 to see the effect of the density on the production of NO. These cells were stimulated with IFN-γ (40 ng/mL). Each condition had been tested with and without LPS.

Experiment 4: Nitric oxide estimation in NIH-3T3 cells with IFN-γ, IL-10, TGF-β and LPS
The timeline for this experiment is shown in **Figure 4.** The cells were seeded in a 6-well plate with a density of $2 \cdot 10^4$ cells/cm^2. First, the cells were incubated for 24h at 37 °C. Next, the medium was removed and new medium was added with the stimulants. The cells were treated with: TGF-β (10 ng/mL), IFN-γ (40 ng/mL), murine IL-10 (30 ng/mL) and solely medium. The cells were incubated for 3 hours. Then, LPS (100 ng/mL) was added to one well of each condition. The cells were incubated for 72 hours. After the incubation period, 250 µL samples were taken from the medium and an NO assay was performed.

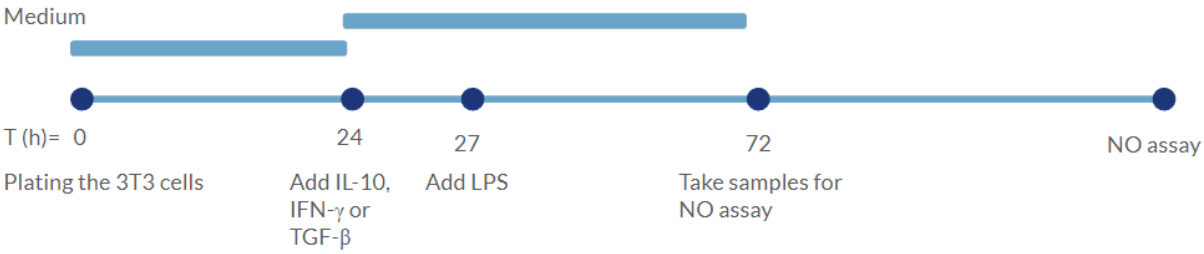

Figure 4: Timeline of NO assay experiment 4, including the stimulation and the time by which the medium is used.

DHPAA-Assay

The timeline for this experiment is shown in **Figure 5.** The NIH-3T3 cells were seeded onto a 6-well plate at three different densities: $3 \cdot 10^4$, 10^4 and $5 \cdot 10^3$ cells/cm^2 (with an incubation time of 24h, 48h and 72h, respectively). First, the cells were incubated for 24h. The medium was removed and new medium was added with stimulants. To stimulate the cells, TGF-β (10 ng/mL) was added to three wells. The other wells solely contained medium. Then, they were incubated for 24h, 48h or 72h. This experiment was performed twice according to the protocol stated in

Appendix D. However, there was a difference in enzymatic degradation time. For the first experiment, an incubation time of 1 hour was used with bacterial collagenase. The second experiment had an incubation time of 20 hours.

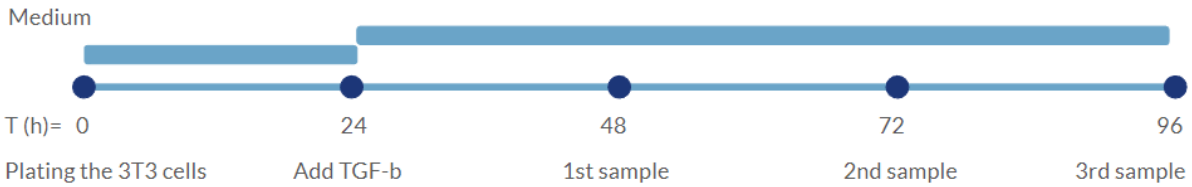

Figure 5: Timeline of DHPAA-assay experiment 1 and 2, including the stimulation and the time by which the medium is used.

Protein assay

To account for the quantity of protein in the samples, a protein assay was performed. With this assay, the amount of protein can be determined relative to a standard, which was Bovine Serum Albumin (BSA) in this case. This assay was performed for both collagen assays according to standard procedures. The full protocol can be found in **Appendix F.**

Quantitative Polymerase Chain Reaction (qPCR)

Culturing the samples

The timeline for this experiment is shown in **Figure 6.** The 3T3 cells were seeded in a 6-wells plate with a density of $4 \cdot 10^4$ cells/cm^2. The cells were incubated for 24 hours at 37 °C. Subsequently, the cells were stimulated with solely medium, TGF-β (10 ng/mL), IFN-γ (40 ng/mL) and murine IL-10 (30 ng/mL). They were incubated for 3 hours. After this, LPS (100 ng/mL) was added to each condition and the cells were incubated for 1 hour. After incubation, the wells plate with the cells were put on ice. The protocol that is stated in **Appendices H, I, J** was used to prepare the samples and perform the qPCR.

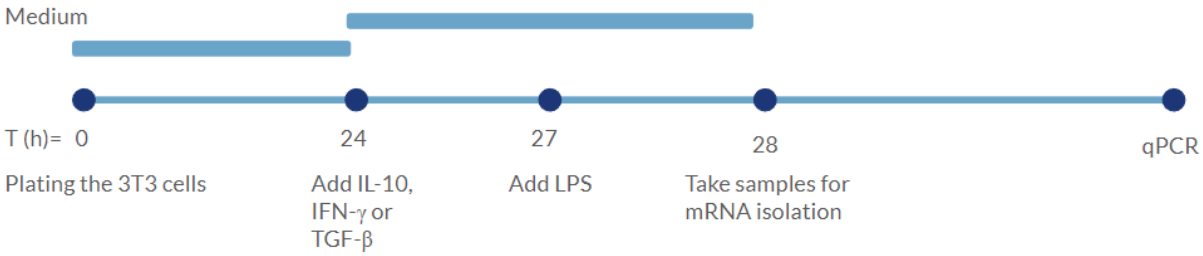

Figure 6: Timeline of the sample preparation for the qPCR, including the stimulation and the time by which the medium is used.

Results and Discussion

All the experiments were also performed by another student. These results are comparable to the ones shown in this report and therefore these are not shown. However, it is noteworthy that each experiment has been performed in duplicate and thus, the results have been reproduced at least once.

Nitric oxide production

The full protocol for the NO assay can be found in **Appendix B.** In **Appendix C**, an example of a standard curve is shown. With this, the nitric oxide concentration was estimated in each experiment.

To guarantee valid results, a positive sample was measured with each NO assay. This sample included RAW cells stimulated with 40 ng/mL IFN-γ (2h) and 100 ng/mL LPS (24h). For each experiment, the positive control gave a positive result, indicating a valid experiment.

Experiment 1

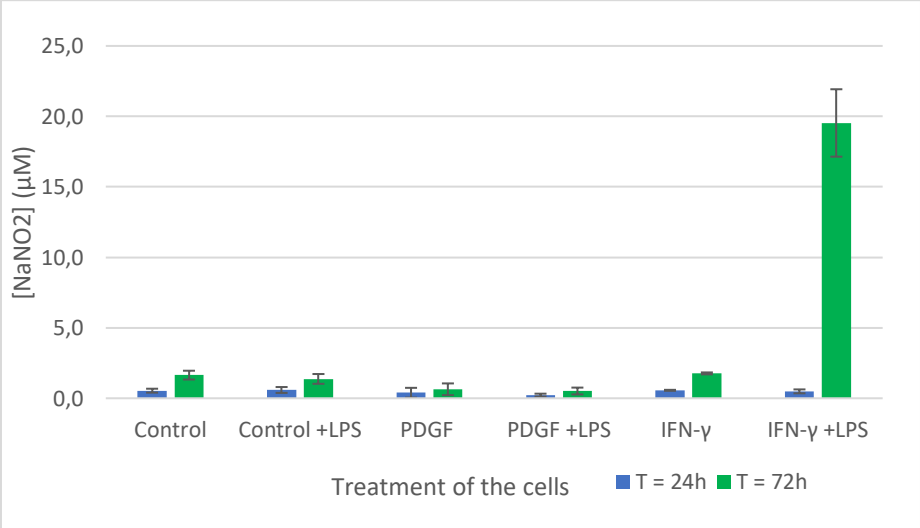

Figure 7: Graph showing the produced [$NaNO_2$] (µM) by NIH-3T3 cells. A control is shown, solely incubated in medium. The other NIH-3T3 cells were treated with: PDGF-β (40 ng/mL), IFN-γ (40 ng/mL) and LPS (100 ng/mL) (24h and 72h stimulation). The raw data is stated in ***Appendix K.***

In **Figure 7,** the results of **experiment 1** can be seen. The cells were stimulated with PDGF-β, IFN-γ and LPS for 24h and 72h. For all samples it can be seen that the NO production is higher when incubated for 72h, compared to 24h. Additionally, LPS does not show a significantly higher $NaNO_2$ concentration in the control and PDGF-β samples. However, It can be seen that LPS shows an increase in NO production when IFN-γ is added and incubated for 72h.

As liver fibrosis is caused by inflammation, it was decided to examine whether inflammation can be measured in fibroblasts by the produced NO. So far there are not many studies that mention fibroblasts producing NO. Therefore, it was chosen to use different stimuli and determine their effect by measuring the excreted NO in the medium. In this experiment, the cells were stimulated with PDGF-β, IFN-γ and LPS (**Figure 7**). As mentioned before, PDGF-β is a well-known growth factor. In this case, it was added as it might give a boost to the effect of LPS as this is pro-inflammatory. The hypothesis is that PDGF-β would increase the cell proliferation and thereby

the NO production when stimulated with LPS. [25] In previous research it had been found that IFN-γ could also enhance the effect of LPS. Therefore, this was also used as a stimulus. [12] To determine the effect of the stimulation time, it was chosen to incubate for 24h and 72h.
As can be seen in **Figure 1**, IFN-γ is able to stimulate NO production with the addition of LPS for 72h. Additionally, it can be concluded that stimulating for 24h with and without LPS, is not enough time for the cells to start producing NO. The results suggest that PDGF does not have an effect on the nitric oxide production of 3T3 cells when stimulated for 24 and 72 hours. Looking at the cells under the microscope, clear effects of PDGF-β were seen. **(Appendix L).** Many clusters were visible and the wells also contained more and larger cells than the others. Thus, PDGF-β did affect the cells but not by inducing nitric oxide release. It could be that a higher dose of PDGF-β is needed or that the cells need to be stimulated for a longer time.

Experiment 2

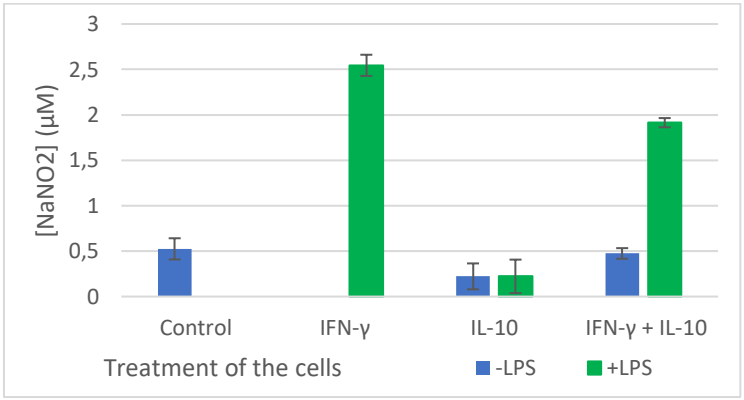

*Figure 8: Graph showing the produced [NaNO2] (µM) by NIH-3T3 cells. A control is shown, solely incubated in medium. The other NIH-3T3 cells were treated with: IFN-γ (40 ng/mL), IL-10 (30 ng/mL), IFN-γ and IL-10 (40 and 30 ng/mL, respectively) and LPS (100 ng/mL). The cells were stimulated for 72h. The raw data is stated in **Appendix K.***

In **Figure 8,** the produced NO by the NIH-3T3 cells is depicted with different treatments. In this case, the cells were stimulated with IFN-γ, IL-10, IFN-γ and IL-10 and LPS. It is evident that treatment with IFN-γ and LPS shows a higher NO production, both with and without IL-10. The addition of IL-10 to IFN-γ and LPS causes a smaller production of NO, compared to IFN-γ and LPS on its own. Next to that, the produced NO is ten times lower compared to **Figure 7.**

The cells were stimulated with IFN-γ (**Figure 8)** as this showed a significant NO production in the first experiment **(Figure 7).** Besides, the cells were stimulated for 72h as this was also determined to give a higher NO concentration and therefore results of higher quality. The cells were seeded with a much lower density than in the first experiment which led to a ten times reduction in NO production. This unintentional difference in protocol is not desired as we want to induce as much inflammation as possible to see more differences between stimulants. More cells can produce more nitric oxide. Therefore $2 \cdot 10^4$ cells/cm^2 is used in the other experiments for the NO assay.
In **Figure 8,** it is clear that IFN-γ again increases the NO production. However, human IL-10 was not able to induce NO production with and without LPS. Looking at the results, it seems that IL-10 reduces the NO production when added with IFN-γ and LPS. As results were not convincing, the test was repeated with the same concentrations. It should be noted that human IL-10 is used on mice 3T3 cells. This could potentially influence the results but the usage of human IL-10 was not noticed until the last NO experiment.

Experiment 3

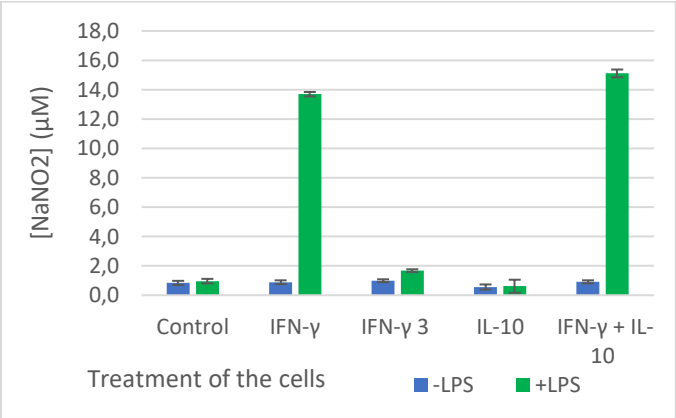

Figure 9: Graph showing the produced [NaNO2] (µM) by NIH-3T3 cells. A control is shown, solely incubated in medium. The other NIH-3T3 cells were treated with: IFN-γ (40 ng/mL), IL-10 (30 ng/mL), IFN-γ and IL-10 (40 and 30 ng/mL, respectively) and LPS (100 ng/mL). All the cells were seeded with a density of 2·104 cells/cm2, except for IFN-γ 3 with a density of 3·103 cells/cm2. The cells were stimulated for 72h. The raw data is stated in ***Appendix K.***

In this experiment, the cells were stimulated with IFN-γ, IL-10, IFN-γ and IL-10 and LPS. To prove that the density caused the difference between experiment 1 and 2, it was tested in experiment 3 (**Figure 9**). The NO concentration is comparable to experiment 1. Comparable to **Figure 7** and **8,** the addition of IFN-γ with LPS causes a high NO production. IFN-γ with LPS at a lower density of cells causes a lower NO concentration, namely 1,7 µg/mL. Again, no significant results were seen from IL-10. Different from **Figure 8**, IFN-γ with IL-10 and LPS shows a higher NO production than IFN-γ with LPS.

It can be concluded that a higher density increases the nitric oxide concentration in the medium. The results in **Figure 8** are contradictory to the results in **Figure 9:** the addition of human IL-10 to IFN-γ and LPS shows a higher NO production than IFN-γ and LPS. Thus, it is not clear what the effect of IL-10 is on the NO production and thereby the induced inflammation in 3T3 cells. Due to an error in experiment 4, we were not able to test IL-10 again in the same circumstances.

Experiment 4

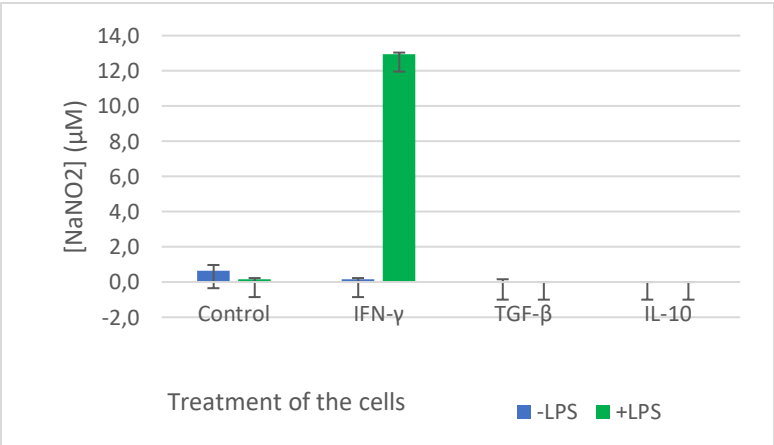

Figure 10: Graph showing the produced [NaNO2] (µM) by NIH-3T3 cells. A control is shown, solely incubated in medium. The other NIH-3T3 cells were treated with: IFN-γ (40 ng/mL), TGF-β (10 ng/mL), IL-10 (30 ng/mL) and LPS (100 ng/mL). The cells were stimulated for 72h. The raw data is stated in ***Appendix K.***

For the final determination of the nitric oxide concentration, the cells were stimulated with IFN-γ, TGF-β, IL-10 and LPS **(Figure 10).** As seen before in **Figure 7, 8 and 9,** IFN-γ with LPS shows the highest NO production. The maximum values are also comparable to in experiment 1, 3 and 4

with 20, 15 and 13 µg/mL, respectively. As the same effect is observed four times, its reproducibility is proven and the results are assumed to be reliable.

TGF-β was used as a stimulus. As mentioned before, this growth factor is a pro-inflammatory protein. [26] However, this cytokine did not induce any measurable nitric oxide release. To know more about the effects of TGF-β, it needs to be tested with a different stimulation time and concentration. Also, we used human TGF-β on a mouse cell line. This might influence the results and therefore, in the future murine TGF-β1 should be used. As said before, PDGF-β was unable to increase the nitric oxide concentration even though it increases cell proliferation. [25]
It is possible that their effect is not measurable by the secretion of nitric oxide. Hence, a different method could be used to test the effect of these stimuli. It is therefore suggested to stimulate the cells with murine TGF-β and PDGF-β with and without LPS to see their effect on the TGF-β and PDGF-β receptor expression and their gene regulation. The receptor expression can be measured by using flow cytometry and the genes can be measured by qPCR. As both factors have a role in collagen production, genes related to this process can be studied.
Interferon gamma was also able to induce nitric oxide release in the last NO assay. Therefore, by all four experiments it can be concluded that interferon is a pro-inflammatory cytokine. Besides, solely LPS is not able to exert its inflammatory effect on 3T3 cells. As NIH-3T3 cells are only one type of fibroblast cell line, the question arises whether the same response will be measured in different fibroblasts, like human fibroblasts.
In this experiment IFN-γ was also tested together with murine IL-10 and LPS. However, due to an error in the procedure, the cells died. Hence, no results are obtained. The effect of IL-10 remains unclear as no significant effects are observed.
We are unable to draw any conclusions on the role of IL-10 on the inflammation of 3T3 cells. It is recommended to test IL-10 again but in a higher concentration. It is also recommended to test it by pre-stimulating the cells with this cytokine and then adding IFN-γ and LPS to see its effect.

As the NO production can be largely influenced by the number of proliferating cells, a cell viability test should be included in the future. An example of this is the 3,[4,5-dimethylthiazol-2-yl]-2,5 diphenyl tetrazolium bromide (MTT) assay. It is based on the conversion of MTT into formazan crystals by living cells. With this, the mitochondrial activity can be determined and this is related to the number of viable cells. [27]

DHPAA-assay

A novel collagen assay has recently been published. It is based on utilizing the formation of a fluorophore complex after the initial enzymatic collagen digestion and fluorophore addition. [28]

The full protocol of the collagen assay is stated in **Appendix D** with an example of a standard curve in **Appendix E**. To quantify the amount of protein that was present, a protein assay was performed **(Figure 12).** The full protocol can be found in **Appendix F** and an example of a standard curve in **Appendix G.**

Experiment 1 **Experiment 2**

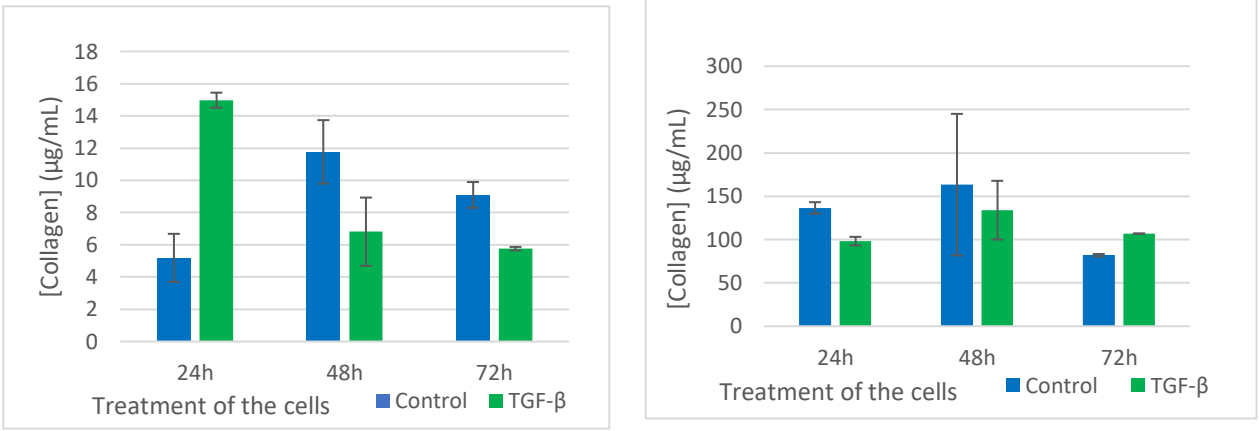

*Figure 11: Graphs showing the measured collagen with the DHPAA-assay in NIH-3T3 cells. The cells were incubated with solely medium or stimulated with TGF-β (10 ng/mL) for 24h, 48h, or 72h. Experiment 1 had an enzymatic degradation time of 1h and experiment 2 had 20h. The raw data is stated in **Appendix M.***

Experiment 1 **Experiment 2**

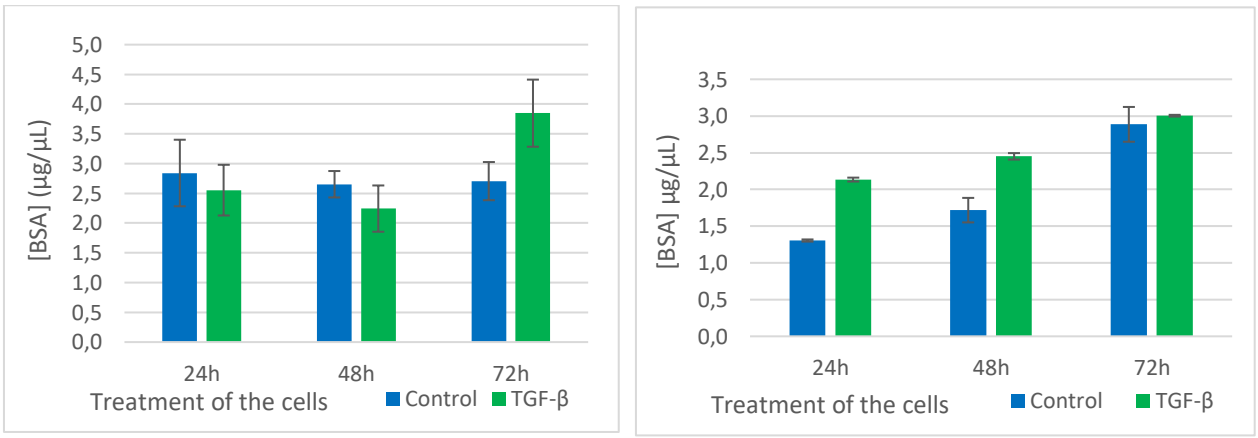

*Figure 12: Graphs showing the measured protein concentration measured with the protein assay. The cells were incubated with solely medium or stimulated with TGF-β (10 ng/mL) for 24h, 48h, or 72h. Experiment 1 had an enzymatic degradation time of 1h and experiment 2 had 20h. The raw data is stated in **Appendix N.***

For this experiment, the collagen concentration was measured by the DHPAA-assay. To determine the effect of the stimulation time, the cells were harvested after 24h, 48h and 72h. The experiment had been performed twice. However, the difference between experiment 1 and 2 is the incubation time with bacterial collagenase. Experiment 1 is incubated for 1h, whereas experiment 2 is incubated for 20h. During the first experiment, a mistake had been made in the protocol during the preparation of the samples for the calibration curve. Thus, the calibration curve from a different plate prepared with the same protocol had been used to calculate the collagen concentrations in experiment 1. This could have influence the results but the ratios are the same.

In **Figure 11** the results of the experiments are shown. Starting of with experiment 1, there is no clear trend visible regarding the control sample. Even though a different calibration curve was used, the results are assumed to be reliable as the exact same protocol was used. The ratios stay the same. At longer incubation times, it seems that TGF-β decreases the collagen concentration. The maximum collagen concentration is 15 µg/mL. Overall, the protein concentrations are comparable.
Experiment 2 is showing different results. No trend can be observed for both the control and TGF-β. It is also noteworthy that there is a high standard deviation for the control 48h. In this experiment the highest measured collagen concentration is 163 µg/mL. Regarding the protein concentrations, both TGF-β and the control get increasingly higher.
Comparing experiment 1 to experiment 2, the collagen concentrations measured in the second experiment are ten times higher than in the first experiment.

The DHPAA-assay was used to determine the effect of different stimuli on the collagen concentration. Due to time restraints, only TGF-β was tested. Regarding the standard curve, the samples of experiment 1 are more on the lower side of the curve with a maximum concentration of 15 µg/mL and experiment 2 is more at the top with a maximum concentration of 163 µg/mL. As only a concentration of 100 and 300 µg/mL is included in the standard curve, the curve is mainly based on the lower concentrations. It is recommended to also include e.g. 150 µg/mL and 200 µg/mL for a more accurate determination of the collagen concentration.

In literature it is stated that TGF-β is able to induce collagen production by promoting the gene expression of different collagen types, namely collagen type I and III. [29] Therefore, this cytokine was used as a positive control. However, in **Figure 11** the effect of TGF-β does not become clear. Keeping the protein concentrations in mind, there is no observable effect for both the control and TGF-β. The results are varying. It could be possible that a higher concentration of TGF-β is needed. Therefore, it could be interesting to test this in the future. As there is collagen measurable and the standard curve showed a linear trend, it is assumed that the assay is well performed and that the solutions were correctly prepared.
Additionally, the incubation time with bacterial collagenase had an influence on the results. Prolonging the incubation period increased the digestion time of the enzyme. This led to a tenfold increase in collagen concentration in experiment 2 compared to experiment 1. Thus, it is recommended to proceed with a 20h incubation period.
The results were comparable to the results of the other student. However, the results are not in line with what is stated in literature. Therefore, it is possible that there are errors in the protocol. In the future, the protocol should be optimized to be able to measure the collagen content accurately. One of the reasons for the results could be that we did not store 3,4-DHPAA properly as it is a fluorescent compound that needs to be stored in the dark. Another reason could be that human TGF-β was used on cells from mice. This can have a different effect than murine TGF-β.

Collagen production is influenced by the amount of cells, the same as with the nitric oxide production. Therefore, a MTT assay should also be included for this assay to normalize for the amount of cells. [27]

qPCR

The detailed protocol used for the determination of the gene expression in NIH-3T3 cells is stated in **Appendices H, I, J**. As some quantities measured in the triplicate deviated more than 0,5 from each other, they were left out in the graph (**Figure 13 and 14**). This was done as the measurements was most likely an error and not an accurate. The negative and positive controls were as expected and therefore the results are assumed to be specific with a valid experimental setup.

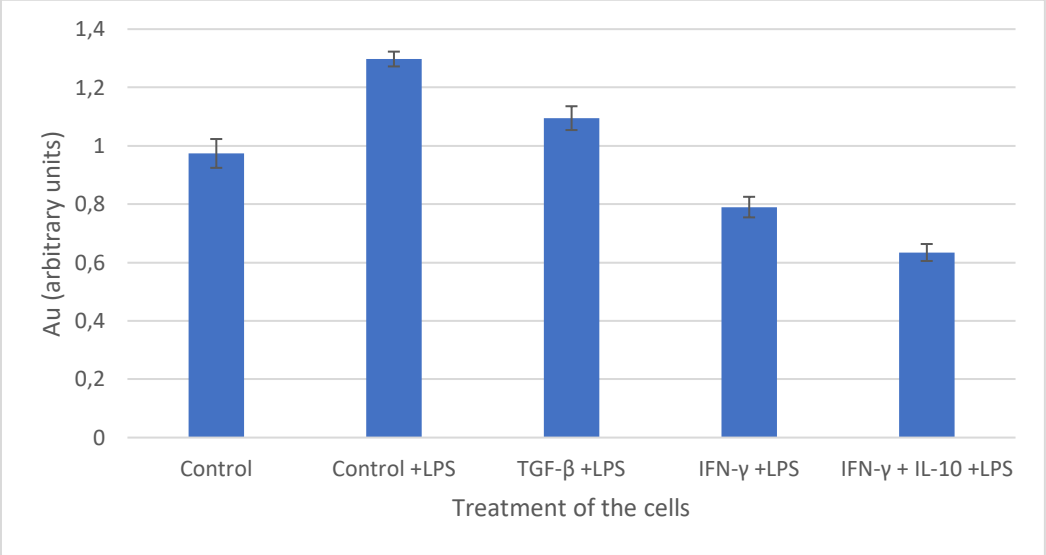

Figure 13: Graph showing the gene expression of β-actin of NIH-3T3 cells. The cells were treated with the following: TGF-β (10 ng/mL), IFN-γ (40 ng/mL), IL-10 (30 ng/mL) and LPS (100 ng/mL). The cells were first stimulated with the cytokines for 3h. The raw data is stated in ***Appendix O.***

In **Appendix O**, the standard curve used for β-actin is shown. **Figure 13** shows the expression of the housekeeping gene beta-actin. The highest expression of β-actin is 1,3 Au and the lowest is 0,6 Au.
As the expression is fluctuating it was decided to not compensate the gene expression of HAS1, 2 and 3 for the housekeeping gene. Compensating would give a wrong impression of the results. Therefore, the question arises whether β-actin is suitable as a house-keeping gene. For future experiments it is suggested to test a different gene, like glyceraldehyde-3-phosphate dehydrogenase (GAPDH). [30]

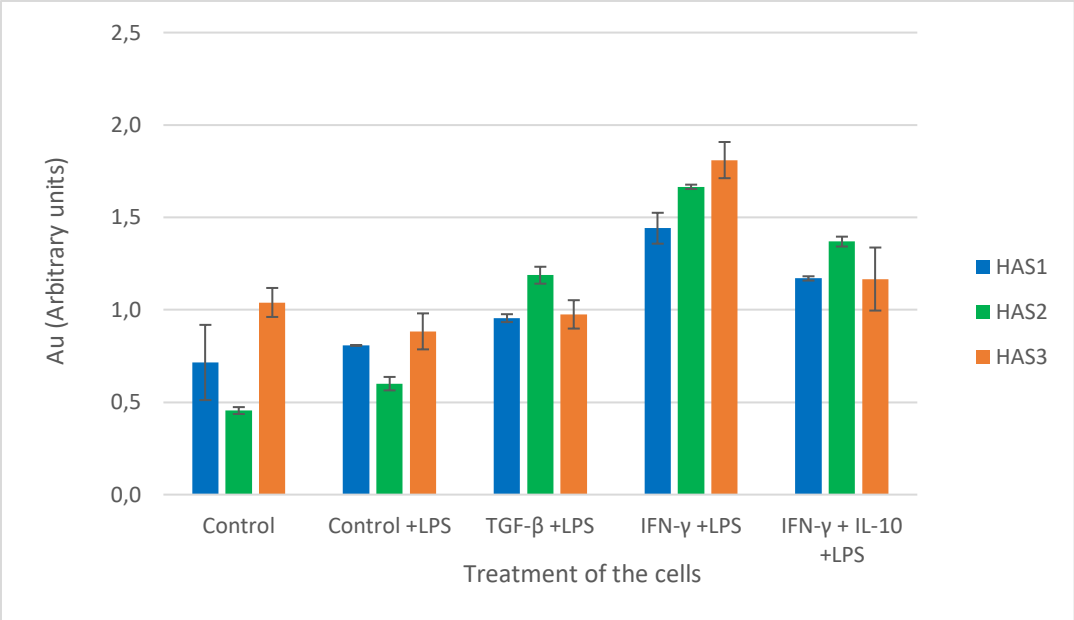

Figure 14: Graph showing the gene expression of HAS1, HAS2, HAS3 of NIH-3T3 cells. The cells were treated with the following: TGF-β (10 ng/mL), IFN-γ (40 ng/mL), IL-10 (30 ng/mL) and LPS (100 ng/mL). The cells were first stimulated with the cytokines for 3h. Then, LPS was added for another hour. The data is not compensated for the housekeeping gene β-actin. The raw data is stated in ***Appendix O.***

In **Figure 14** the gene expression of HAS1, 2 and 3 by NIH-3T3 cells is shown. The cells were treated with TGF-β, IFN-γ, IFN-γ and IL-10 and LPS.

For each gene, the addition of IFN-γ leads to the highest gene expression. Adding IL-10 to IFN-γ leads to a lower gene expression in each gene. Adding TGF-β and solely LPS did not cause any significant effects.

As explained before, a higher amount of hyaluronic acid leads to a more flexible ECM. This is also induced by inflammation to allow the infiltration of immune cells. [31] Fibrosis is characterized by a lower amount of hyaluronic acid, leading to stiff scar tissue. As hyaluronic synthase produces hyaluronic acid, it is expected that an increase in HAS gene expression leads to an increase in hyaluronic acid. However, this is not yet proven and can therefore not be assumed.
In this experiment, TGF-β was added to study its potent pro-fibrotic effects [32] In **Figure 14**, there is no significant upregulation of HAS visible, compared to the control. This can be explained by the fact that fibrosis has less hyaluronic acid present in the ECM and therefore less hyaluronic synthase is needed.
Furthermore, IFN-γ was added to study its anti-fibrotic effects on the gene expression. As said before, IFN-γ is also pro-inflammatory. In the results it becomes clear that IFN-γ upregulates the expression of HAS1, 2 and 3. It is expected that due to the pro-inflammatory effects of IFN-γ, HAS is upregulated to make the tissue more loose for the infiltration of immune cells.
Lastly, IL-10 was added to IFN-γ and LPS. Each gene shows a lower expression compared to IFN-γ and LPS. Thus, it seems that IL-10 is reducing HAS expression. This could be due to the anti-inflammatory effects of IL-10. However, the housekeeping gene is unstable. Hence, the experiment should be repeated with the same circumstances but a stable housekeeping gene to normalize the data and ensure accurate gene expression.

For the future, it is suggested to test IFN-γ again with and without IL-10. This includes testing pre-stimulating with IL-10. Due to time restraints it was not possible to solely test IL-10 in this experiment. Therefore, it is highly recommended to include IL-10 with LPS.

Overall, IFN-γ has played a very important role in this study. This cytokine showed its inflammatory effects by the increase in nitric oxide production by fibroblasts. Besides, the HAS gene expression is upregulated with the stimulation of interferon gamma. After optimizing the DHPAA-assay, the effect of IFN-γ on the collagen concentration can also be tested.
The collagen assay did not show results we hoped for. However, the standard curve was measurable..
The effects of interleukin-10 remain debatable. qPCR showed the most promising results for IL-10 where the same effect was visible for each gene. Therefore, this might be a method for future research against liver fibrosis.

Conclusion

The nitric oxide assay showed that NIH-3T3 cells are able to produce NO when stimulated with IFN-γ and LPS. This is in line with the literature. It can be concluded that the NO assay can be used to measure the NO produced by fibroblasts. Addition of IL-10 did not cause a significant effect. Other stimulants like PDGF-β and TGF-β were also unable to show a response.

Regarding the collagen assay, increasing the digestion time of the enzyme, increased the collagen production. Because of the inconsistent results of the DHPAA-assay, nothing can be concluded about the collagen production. However, the calibration curve was reproducible. After optimizing the assay, it is expected that the assay can be used to measure samples. It is recommended to test the effect of TGF-β and IFN-γ on the collagen production of fibroblasts.

Quantitative PCR was used to measure the gene expression of HAS1, 2 and 3 with β-actin as housekeeping gene. No clear effects of TGF-β were observed. IFN-γ and LPS were able to increase the expression of all the fibrogenic gene markers. In all genes, IL-10 reduced the effect of IFN-γ and LPS in fibroblasts possibly explained by its anti-inflammatory function. As this has only been performed once, further experiments need to be conducted for any conclusions. Furthermore, as the results of the housekeeping gene were fluctuating, the results could not be normalized. Thus, a different housekeeping gene should be used for a better interpretation of the results.

Knowing the mechanism behind IL-10 will give insights into the potential of this cytokine against liver fibrosis. This disease includes many different processes like the growth of fibroblasts, deposition of fibrous connective tissue and the infiltration of inflammatory cells. Interleukin 10 showed its anti-inflammatory properties through qPCR but no anti-fibrotic effects were observed. Interferon-gamma revealed the most promising results in this study due to its pro-inflammatory effect on both the nitric oxide concentration and HAS gene expression. Exploring how interferon gamma and IL-10 work together could shed new light on multiple aspects of liver fibrosis. This contributes to finding the answer to the main question of this study. So far, the potential anti-fibrotic effects of IL-10 on stimulated fibroblasts remain uncertain.

References

1. Acharya, P., Chouhan, K., Weiskirchen, S., & Weiskirchen, R. (2021). Cellular Mechanisms of Liver Fibrosis. Frontiers in pharmacology, 12, 671640. https://doi.org/10.3389/fphar.2021.671640
2. Carlessi R, Köhn-Gaone J, Olynyk JK, et al. (Oct 24 2019) Mouse Models of Hepatocellular Carcinoma. In: Tirnitz-Parker JEE, editor. Hepatocellular Carcinoma [Internet]. Brisbane (AU): Codon Publications; Figure 1 Available from: https://www.ncbi.nlm.nih.gov/books/NBK549197/figure/Ch4-f0001/ doi: 10.15586/hepatocellularcarcinoma.2019.ch4
3. Zhang, D., Zhang, Y. and Sun, B. (2022) 'The molecular mechanisms of liver fibrosis and its potential therapy in application', International Journal of Molecular Sciences, 23(20), p. 12572. doi:10.3390/ijms232012572.
4. Wang, F.-D., Zhou, J. and Chen, E.-Q. (2022) 'Molecular mechanisms and potential new therapeutic drugs for liver fibrosis', Frontiers in Pharmacology, 13. doi:10.3389/fphar.2022.787748.
5. D'Urso, M. and Kurniawan, N.A. (2020) 'Mechanical and physical regulation of fibroblast–myofibroblast transition: From cellular mechanoresponse to tissue pathology', *Frontiers in Bioengineering and Biotechnology*, 8. doi:10.3389/fbioe.2020.609653.
6. Mattos Pinto, A. (2013). Redirecting interleukin-10 in the fibrotic liver: effects on the pathogenesis. s.n]
7. Qin, R. et al. (2022) 'Indole-based small molecules as potential therapeutic agents for the treatment of fibrosis', Frontiers in Pharmacology, 13. doi:10.3389/fphar.2022.845892.
8. Xu, R., Zhang, Z. and Wang, F.-S. (2011a) 'Liver fibrosis: Mechanisms of immune-mediated liver injury', *Cellular & Molecular Immunology*, 9(4), pp. 296–301. doi:10.1038/cmi.2011.53.
9. Tucureanu, M. M., Rebleanu, D., Constantinescu, C. A., Deleanu, M., Voicu, G., Butoi, E., Calin, M., & Manduteanu, I. (2017). Lipopolysaccharide-induced inflammation in monocytes/macrophages is blocked by liposomal delivery of G_i-protein inhibitor. International journal of nanomedicine, 13, 63–76. https://doi.org/10.2147/IJN.S150918]
10. Li, X. P., Liu, P., Li, Y. F., Zhang, G. L., Zeng, D. S., & Liu, D. L. (2019). LPS induces activation of the TLR4 pathway in fibroblasts and promotes skin scar formation through collagen I and TGF-β in skin lesions. International journal of clinical and experimental pathology, 12(6), 2121–2129.]
11. Sharma, J. N., Al-Omran, A., & Parvathy, S. S. (2007). Role of nitric oxide in inflammatory diseases. Inflammopharmacology, 15(6), 252–259. https://doi.org/10.1007/s10787-007-0013-x
12. Wang, R., Ghahary, A., Shen, Y. J., Scott, P. G., & Tredget, E. E. (1996). Human dermal fibroblasts produce nitric oxide and express both constitutive and inducible nitric oxide synthase isoforms. The Journal of investigative dermatology, 106(3), 419–427. https://doi.org/10.1111/1523-1747.ep12343428]

13. Steen, E. H., Wang, X., Balaji, S., Butte, M. J., Bollyky, P. L., & Keswani, S. G. (2020). The Role of the Anti-Inflammatory Cytokine Interleukin-10 in Tissue Fibrosis. Advances in wound care, 9(4), 184–198. https://doi.org/10.1089/wound.2019.1032]
14. Bhat, M. Y., Solanki, H. S., Advani, J., Khan, A. A., Keshava Prasad, T. S., Gowda, H., Thiyagarajan, S., & Chatterjee, A. (2018). Comprehensive network map of interferon gamma signaling. Journal of cell communication and signaling, 12(4), 745–751. https://doi.org/10.1007/s12079-018-0486-y.]
15. Tau, G., & Rothman, P. (1999). Biologic functions of the IFN-gamma receptors. Allergy, 54(12), 1233–1251. https://doi.org/10.1034/j.1398-9995.1999.00099.x
16. Griffin, D.E. (2008) 'Cytokines and chemokines', Encyclopedia of Virology, pp. 620–624. doi:10.1016/b978-012374410-4.00374-5.
17. Vu, T.N., Chen, X., Foda, H.D. *et al.* Interferon-γ enhances the antifibrotic effects of pirfenidone by attenuating IPF lung fibroblast activation and differentiation. *Respir Res* 20, 206 (2019). https://doi.org/10.1186/s12931-019-1171-2]
18. Ricard-Blum S. (2011). The collagen family. Cold Spring Harbor perspectives in biology, 3(1), a004978. https://doi.org/10.1101/cshperspect.a004978]
19. Garantziotis, S., & Savani, R. C. (2019). Hyaluronan biology: A complex balancing act of structure, function, location and context. Matrix biology : journal of the International Society for Matrix Biology, 78-79, 1–10. https://doi.org/10.1016/j.matbio.2019.02.002]
20. Knudson CB, Knudson W. 2001. Cartilage proteoglycans. Seminars in Cell & Developmental Biology. 12(2):69-78. https://doi.org/10.1006/scdb.2000.0243
21. lberts B, Bray D, Johnson A, Lewis J, Walter P, Raff M, Roberts K. 1988. Essential Cell Biology: An Introduction to the Molecular Biology of the Cell Garland Pub
22. Itano, N., Sawai, T., Yoshida, M., Lenas, P., Yamada, Y., Imagawa, M., Shinomura, T., Hamaguchi, M., Yoshida, Y., Ohnuki, Y., Miyauchi, S., Spicer, A. P., McDonald, J. A., & Kimata, K. (1999). Three isoforms of mammalian hyaluronan synthases have distinct enzymatic properties. The Journal of biological chemistry, 274(35), 25085–25092.
23. HAS1 and HAS2 produce high molecular weight HA and HAS3 produces low molecular weight HA. [Stern, R. (2009) Hyaluronan in cancer biology. Amsterdam, Netherlands: Elsevier Academic Press.
24. Jung, M., Ma, Y., Iyer, R. P., DeLeon-Pennell, K. Y., Yabluchanskiy, A., Garrett, M. R., & Lindsey, M. L. (2017). IL-10 improves cardiac remodeling after myocardial infarction by stimulating M2 macrophage polarization and fibroblast activation. Basic research in cardiology, 112(3), 33. https://doi.org/10.1007/s00395-017-0622-5
25. Kardas, G., Daszyńska-Kardas, A., Marynowski, M., Brząkalska, O., Kuna, P., & Panek, M. (2020). Role of Platelet-Derived Growth Factor (PDGF) in Asthma as an Immunoregulatory Factor Mediating Airway Remodeling and Possible Pharmacological Target. *Frontiers in pharmacology*, *11*, 47. https://doi.org/10.3389/fphar.2020.00047
26. Sanjabi, S., Zenewicz, L. A., Kamanaka, M., & Flavell, R. A. (2009). Anti-inflammatory and pro-inflammatory roles of TGF-beta, IL-10, and IL-22 in immunity and autoimmunity. *Current opinion in pharmacology*, *9*(4), 447–453. https://doi.org/10.1016/j.coph.2009.04.008]
27. van Meerloo, J., Kaspers, G. J., & Cloos, J. (2011). Cell sensitivity assays: the MTT assay. *Methods in molecular biology (Clifton, N.J.)*, *731*, 237–245. https://doi.org/10.1007/978-1-61779-080-5_20

28. Yasmin, H., Kabashima, T., Rahman, M. S., Shibata, T. & Kai, M. Amplified and selective assay of collagens by enzymatic and fluorescent reactions. Sci Rep 4, (2014).
29. Lijnen, P., & Petrov, V. (2002). Transforming growth factor-beta 1-induced collagen production in cultures of cardiac fibroblasts is the result of the appearance of myofibroblasts. *Methods and findings in experimental and clinical pharmacology*, *24*(6), 333–344.
30. Barber, R. D., Harmer, D. W., Coleman, R. A., & Clark, B. J. (2005). GAPDH as a housekeeping gene: analysis of GAPDH mRNA expression in a panel of 72 human tissues. *Physiological genomics*, *21*(3), 389–395. https://doi.org/10.1152/physiolgenomics.00025.2005
31. Marinho, A., Nunes, C., & Reis, S. (2021). Hyaluronic Acid: A Key Ingredient in the Therapy of Inflammation. *Biomolecules*, *11*(10), 1518. https://doi.org/10.3390/biom11101518
32. Frangogiannis N. (2020). Transforming growth factor-β in tissue fibrosis. *The Journal of experimental medicine*, *217*(3), e20190103. https://doi.org/10.1084/jem.20190103

Appendix

Appendix A: Protocol for cell culturing

Solutions:

- Dulbecco's Modified Eagle's Medium (DMEM) with 10% Fetal Bovine Serum at 37 °C.
- Phosphate buffered saline (PBS) at 37 °C
- trypsin (TEP) at room temperature

Each solution was stored at 4 °C.

Procedure

- For cell culturing, make sure the cells are viable by looking at them microscopically in the T25 flask (surface area = 25 cm^2).
- Then, remove the old 3T3 medium from the cultured cells.
- Wash the cells twice with 5 mL PBS and remove PBS in between the washing steps. Do not add PBS directly onto the cells.
- Pipet 750 µL TEP onto the cells and wait for the cells to detach from the bottom of the plate.
- Pipet 5 mL 3T3 medium onto the cells and resuspend the solution.
- Pipet the solution in a 15 mL tube.
- Pipet 9 µL of the suspension in a hemocytometer and count the cells.
- Calculate the suspension needed for culturing a specific density according to their incubation time:
    - 2 days: 10^4 cells/cm^2
    - 3 days: $3 \cdot 10^3$ cells/cm^2
    - 4 days: $5 \cdot 10^3$ cells/cm^2
- Pipet 5 mL 3T3 medium in the new T25.
- Add the calculated amount of suspension, after resuspending, to the T25 flask.
- Incubate the cells accordingly at 37 °C.

Appendix B: protocol for NO assay

Solutions:

- A stock solution of 100 mM $NaNO_2$ in MQ (0,69 g/100 mL) is used (store vials at -20 °C).
- Dilute the $NaNO_2$ stock solution 100x in DMEM for a 1 mM solution.
- Griess reagent A: add 2 grams of sulphanilamide and 5 mL phosphoric acid to 100 mL MQ water (used and stored at room temperature)
- Griess reagent B: add 200 mg N-(1-Naphthyl)ethylenediamine dihydrochloride to 100 mL MQ water (used and stored at room temperature).

Procedure

- For the standard curve, prepare the concentrations $NaNO_2$ as stated in **Table1**

Table 1: pipetting scheme of the calibration curve used for the NO estimation of NIH-3T3 cells.

[$NaNO_2$] (µM)	**Volume $NaNO_2$**	**Volume medium**
100	100 µL 1 mM	900 µL
50	500 µL 100 µM	500 µL
25	500 µL 50 µM	500 µL
12,5	500 µL 25 µM	500 µL
6,3	500 µL 12,5 µM	500 µL

3,1	500 µL 6,3 µM	500 µL
1,6	500 µL 3,1 µM	500 µL
0,8	500 µL 1,6 µM	500 µL
0	-	500 µL

- For the reaction, pipet 100 µL of the standard curve samples in triplicate in a 96 wells plate.
- Pipet 100 µL of the experimental samples in empty wells.
- Prepare fresh Griess reagent by mixing equal volumes of Griess A and Griess B.
- Add 100 µL of the prepared Griess to each standard and sample.
- Remove bubbles from the wells
- Measure the absorbance at 550 nm in the spectrophotometer.

Appendix C: Standard curve NO assay

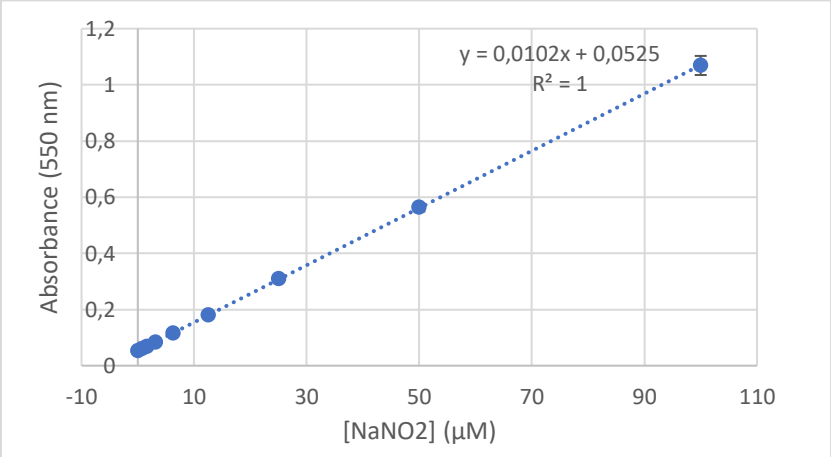

Figure 15: *Graph showing an example of a standard curve that is used to calculate the production of nitric oxide by NIH-3T3 cells. The formula of the trendline is shown.*

In **Figure 15,** a standard curve is shown by which the nitric oxide concentration is calculated. A linear trend is visible and the corresponding formula is:
$y = 0{,}102x + 0{,}5025$
The measured absorbance for the samples can be filled into the formula as y, giving x which is the concentration of NO. An example is shown below with an absorbance of 0,6.

$$0{,}6 = 0{,}102x + 0{,}5025$$

$$x = \frac{0{,}6 - 0{,}5025}{0{,}102} = 0{,}96\ \mu M\ NaNO_2$$

Appendix D: protocol for DHPAA-assay

Solutions:

- Phosphate Buffered Saline (PBS) (stored at 4 °C)
- Trypsin (TEP) (stored at 4 °C)
- MQ water
- 50 mM tris buffer (pH = 7.5)
- 0,1 mg/mL bacterial collagenase (stored at -20 °C)
    - Dissolve bacterial collagenase in 50 mM tris buffer (pH = 7.5)

    - 0,55 gr $CaCl_2$ (5 mm)
    - Do not vortex!
- 125 mM sodium borate buffer (pH = 7.5) (stored at 4 °C)
    - 0,0775 gr Boric acid
    - 10 mL demi water
    - 5,55 mg $CaCl_2$
    - 12,5 mg NaOH
    - Adjust pH to 7.5
- 5 mM sodium borate buffer (pH = 7.5) (stored at 4 °C)
    - 0,310 gr Boric acid
    - 10 mL demi water
    - 2,22 mg $CaCl_2$
    - 12,5 mg NaOH
    - Adjust pH to 7.5
- 125 mM Borate (pH = 8.0) (stored at 4 °C)
    - Dissolve 0,310 gr boric acid in 40 mL H_2O
    - 50 mg NaOH
    - Adjust pH to 8.0
- 1,25 mM sodium periodate($NaIO_4$) (stored at 4 °C)
    - 10,7 mg $NaIO_4$
    - 40 mL demi water
- 0,75 mM 3,4-Dihydroxyphenylacetic acid (3,4-DHPAA) (stored at 4 °C with aluminium foil)
    - 5,05 mg DHPAA
    - 40 mL demi water
- Collagen from rattail type I à 4,24 mg/mL stock solution

Procedure

Cell preparation

- Seed the NIH-3T3 cells in a 6-wells plate with the density according to their incubation time as stated in **Table 2** . Each incubation time has 2 wells.
- Incubate the cells for 24h.
- Remove the old medium and add new medium. Add TGF-β (10 ng/mL) to 3 wells.
- Incubate the cells according to their density

Table 2: The incubation time and density of the NIH-3T3 cells used in the DHPAA-assay.

Incubation time	**Density**
24h	$3 \cdot 10^4$ cells/cm^2
48h	10^4 cells/cm^2
72h	$5 \cdot 10^3$ cells/cm^2

Harvesting the cells

- Remove the medium from the cells
- Wash twice with 1000 µL phosphate buffered saline (PBS)
- Add 400 µL TEP to the wells
- Add 1,6 mL medium when the cells are detached from the well

- Take the medium form the well and pipet into separate tubes
- Centrifuge the cells for 5 minutes at 300 rpm.
- Remove the supernatant
- Store the pellet at -80 °C until further use.

Enzymatic degradation

- Prepare the solutions needed for the collagen assay and store them accordingly.
- Add 200 µL MQ water to the pellet and homogenize with a micro homogenizer.
- Take 100 µL of the sample
- Add:
    - 20 µL bacterial collagenase (0,1 mg/mL)
    - 100 µL of 125 mM borate buffer (5 mM $CaCl_2$, pH = 7.5)
    - 30 µL MQ water
- Mix the solution, do not vortex!
- Incubate the samples for 1 hour or 20 hours at 37 °C
- Centrifuge the samples for 5 minutes at 14.000 rpm.

Fluorescence detection

- Take 200 µL supernatant to perform further experiments
- Add:
    - 250 µL 0.75 mM 3,4-DHPAA
    - 250 µL 125 mM Borate (5 mM $CaCl_2$, pH = 8.0)
    - 250 µL of 1.25 mM $NaIO_4$
- Vortex the solution
- To form the fluorophore, incubate for 10 minutes at 37 °C
- Pipet 200 µL of the samples in a 96-well black plate
- Prepare the concentrations for the standard curve as stated in **Table 3.**
- Pipet 200 µL of the standard curve in the same 96-well black plate
- Measure the fluorescence intensity (emission = 465 nm, excitation = 375 nm)

Table 3: Pipetting scheme of the calibration curve used for the collagen estimation of NIH-3T3 cells.

[Collagen] (µg/mL)	**Collagen stock (4 mg/mL) (µL)**	**Multi-Q water (µL)**
0	-	2000 µL
1	5 µL	1995 µL
3	15 µL	1985 µL
10	50 µL	1950 µL
30	150 µL	1850 µL
100	500 µL	1500 µL
300	1500 µL	500 µL

Appendix E: Standard curve DHPAA-assay

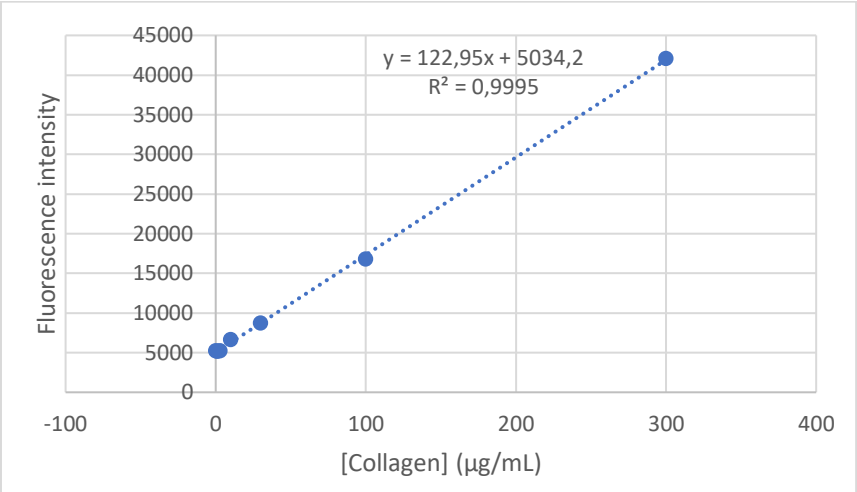

Figure 16: Graph showing an example of a standard curve that is used to calculate the collagen concentration by NIH-3T3 cells. The formula of the trendline is shown.

In **Figure 16,** a standard curve is shown by which the collagen concentration is calculated. A linear trend is visible and the corresponding formula is:
$y = 122{,}95x + 5034{,}2$
The measured fluorescence of the samples can be filled into the formula as y, giving x which is the concentration of collagen. An example is shown below with a fluorescence of 9018.

$$9018 = 122{,}95x + 5034{,}2$$

$$x = \frac{9018 - 5034{,}2}{122{,}95} = 32{,}4\ \mu g/ml\ Collagen$$

Appendix F: protocol for Protein Assay Bio Rad

Solutions:

- Reagent A: 250 mL alkaline copper tartrate solution
- Reagent S: 5 mL surfactant solution
- Reagent B: 1 L dilute Folin reagent
- Stock BSA (Cat nr: A6003): 20 µg/µL

Procedure

- Pipet in triplicate 5 µL of the standard concentration in the wells of a microplate (**Table 4**)
- Pipet in triplicate µL of the samples in empty wells on the same plate
- Pipet in triplicate 5 µL H_2O (background measurement)
- Prepare reagent AS: add 20 µL of assay reagent S per 1 mL of reagent A
- Add to each well 25 µL AS
- Add 200 µL of reagent B per well
- Incubate 15 minutes at room temperature
- Measure the absorbance of the samples at 750 nm
- Calculate the protein concentration of the samples by interpolation in the standard curve.

Table 4: Pipetting scheme of the calibration curve used for the protein estimation of NIH-3T3 cells.

Standard (µg/µL)	BSA	Demi water (µL)
10	20 µL of 20 µg/µL	20
8	16 µL of 20 µg/µL	24
6	12 µL of 20 µg/µL	28
4	8 µL of 20 µg/µL	32
3	6 µL of 20 µg/µL	36
2	4 µL of 20 µg/µL	76
1	4 µL of 20 µg/µL	40
0.5	40 µL of 1 µg/µL	40
0.25	40 µL of 0.5 µg/µL	40
0.125	40 µL of 0.25 µg/µL	40
0.06	40 µL of 0.125 µg/µL	40
0.03	40 µL of 0.06 µg/µL	40

Appendix G: Standard curve Protein Assay

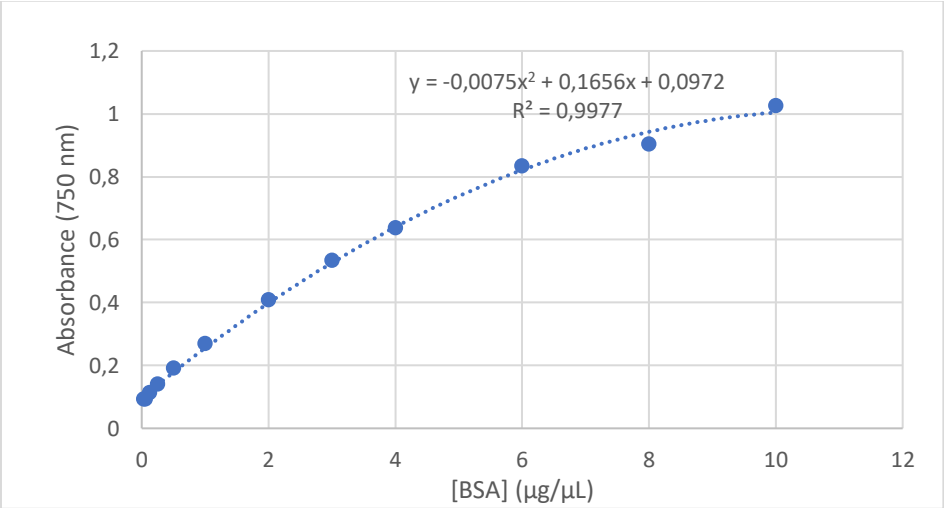

***Figure 17**: Graph showing an example of a standard curve that is used to calculate the protein concentration by NIH-3T3 cells. The formula of the trendline is shown.*

In **Figure 17**, the standard curve of a protein assay is shown with a polynomial trendline. The corresponding formula is:

$$y = -0{,}0075x^2 + 0{,}1656x + 0{,}0972$$

The measured absorbance of the samples can be filled into the formula as y, giving x. This gives the protein concentration of the samples. An example is shown below with an absorbance of 0,3

$$0{,}3 = -0{,}0075x^2 + 0{,}1656x + 0{,}0972$$

$$x = \frac{(-0{,}1656 + (\sqrt{(0{,}1656)^2 - (4 * -0{,}0075 * (0{,}0972 - 0{,}3))}}{2 * -0{,}0075} = 1{,}30\ \mu g/\mu l\ BSA$$

Appendix H: protocol for RNA isolation

RNA Isolation Protocol (Maxwell)

Prepare before starting:

- HB solution: Add 20 µl 1-Thioglycerol per 1 ml of Homogenization Solution.

Harvest the samples:

- Wash the cells twice with PBS and discard the PBS
- Add 100 µl pre-chilled HB to each well, homogenize them with the pipet
- Combine the wells with the same treatment to obtain a higher cell count
- Place the samples in RNase free 1.5 ml tubes on ice

Prepare Maxwell for isolation:

- Place the cartridge (RNA LEV Simple) in the black holder
- Strip off the covers
- Place plungers in position 8
- Add 5 µl DNase (stored at -20) to position 4 (yellow solution), and the solution will turn green
- Place 0.5 ml tubes (from the kit!) in the FRONT row (firmly press tubes)
- Add 40 µl RNase free water in the 0.5 ml tubes (check if there are NO air on the bottom of the tubes)

Lyse the samples:

- Add per sample 200 µl lysis buffer and vortex immediately for 15 seconds.
- Pipet the sample straight in its position in the RNA cartridge.

Start Isolation:

- Turn on the Maxwell → click RUN →
- Choose program 1 → RNA → Simply RNA
- Choose Run (green button) → open the door → place the cartridge in position

Appendix I: protocol for RNA conversion to cDNA

This protocol can be used after the RNA isolation with the Maxwell.

Materials:

- M-MLV Rev Transcriptase
  Cat. nr: M1705 (= 5 * 10.000 units)
- Rnasin
  Cat. nr: N2515 (= 10.000 units)
- Random Hexamers
  Cat. nr: C1181 (=20 µg)
- dNTP's, dATP, dCTP, dGTP, dTTP set 100 µM/nucl.
  Cat. nr: U1245

Precaution:

Tubes, tips and water must be RNase free

You yourself are the source of RNase

Nanodrop

- Measure the samples in the Nanodrop to obtain the concentration of RNA
- Note the purity of the sample by the absorbance ratio A260/A280

- Adjust the concentration to obtain the RNA yield as stated in **Table 5** to pipet a volume of 5 µL in the RT mix

Table 5: Table showing the amount of cells used to obtain the RNA yield.

	Cells/cm²	**Confluency**	**RNA yield (ng/µL)**
3T3 6 well (10 cm²)	$4 \cdot 10^4$	80-90	113-179

Prepare the RT mix according to the quantities as stated below. The quantities are given for a single sample. Prepare the master mix for the number of samples + (5) samples for the calibration curve.

RT mix:	µL per sample	
- RT buffer	2.0 µL	
- dNTP	0.1 µL	
- Rnasin	0.25 µL	(= 10 units)
- Rev Transcriptase	0.5 µL	(= 100 units)
- Random Hexamers	0.5 µL	(= 0.5 µg)
- RNA	0.5 µg	(preferably in 5 µL)
- H_2O	1.65 µL	(to get a total volume of 10 µL)
	---------- +	
➔ Total volume:	10 µL	

Converting RNA to cDNA:

- 10 min 20 °C
- 30 min 42 °C
- 10 min 20 °C
- 5 min 99 °C
- 5 min 20 °C

Place the tubes in the PCR machine
Start the file ***MLVCDNA***
After the reaction is completed:

- Spin the tubes (condensed water from the lids)
- Store the samples at -20 °C

Appendix J: protocol for qPCR

Creating standard curve:

- Pool the undiluted cDNA of the samples that are assigned for the STD curve (**Table 6**)
- Create the Standard Curve according to the table below

Table 6: Table showing the used volumes for the standard curve of the cDNA.

STD (rel)	**V (µL)**	**H_2O (µL)**
STD 4	50 µL of pooled cDNA	75
STD 2	50 µL of STD 4	50
STD 1	50 µL of STD 2	50
STD 0.5	50 µL of STD 1	50
STD 0.25	50 µL of STD 0.5	50

Prepare the cDNA:

- Dilute the cDNA after the conversion 10 times:
    - Add 90 µL RNase free H_2O to the cDNA samples

Prepare 10 µM primermix F+R:

- 20 µL of 50 µM primer For
- 20 µL of 50 µM primer Rev
- 60 µL H_2O

Design the 384 plate layout of the samples digital

Prepare the Taq MasterMix:	µL per sample
Sybr Green Mix	5
Primermix F+R (10 µM)	0.3
Water	2.7
	----- +
Total	8

Prepare the qPCR reaction

- Pipet 2 µL of the standard in triplicate in the 384 wells plate
- Pipet 2 µL of the diluted samples in triplicate in the 384 wells plate
- Add a PC and NC to the plate
- Add 8 µL of the Taq MasterMix to all the wells
- Place a seal on the plate and tight it well
- Go to the PCR machine and start the PCR

PCR protocol:

Stage 1:	10 min	95	Activation Taq
Stage 2:	15 sec	95	Amplification
	30 sec	60	
	40 cycles		
Stage 3:	15 sec	95	Melt curve
	1 min	60	
	Gradient from 0.05/sec to 95		

Appendix K: Raw data NO assay

*Table 7: Table showing the raw data of the standard curve of the NO assay that is shown in **Appendix C**.*

$NaNO_2$ concentration (µg/mL)	Absorbance 1	Absorbance 2	Average absorbance	St Dev
100	1,045	1,093	1,069	0,033941125
50	0,553	0,573	0,563	0,014142136
25	0,308	0,309	0,3085	0,000707107
12,5	0,177	0,183	0,18	0,004242641
6,3	0,114	0,117	0,1155	0,00212132
3,1	0,084	0,084	0,084	0
1,6	0,068	0,068	0,068	0
0,8	0,06	0,061	0,0605	0,000707107
0	0,052	0,052	0,052	0

*Table 8: Absorbance and concentration NO assay experiment 1 (**Figure 7**) T = 24 and 72h, respectively.*

Treatment 24h	Absorbance 1	Absorbance 2	Average absorbance	Average concentration NO (µg/mL)	St Dev
Control	0,06	0,058	0,059		
Control 2	0,056	0,058	0,057	0,539215686	0,138648388
Control +LPS	0,057	0,057	0,057		
Control 2 +LPS	0,06	0,06	0,06	0,588235294	0,207972583
PDGF-β	0,064	0,054	0,059		
PDGF-β 2	0,054	0,054	0,054	0,392156863	0,346620971
PDGF-β +LPS	0,054	0,054	0,054		
PDGF-β 2 +LPS	0,055	0,056	0,056	0,220588235	0,103986291
IFN-γ	0,059	0,058	0,059		
IFN-γ 2	0,059	0,057	0,058	0,56372549	0,034662097
IFN-γ +LPS	0,056	0,057	0,057		
IFN-γ 2 +LPS	0,058	0,059	0,059	0,490196078	0,138648388

Treatment 72h	Absorbance 1	Absorbance 2	Average absorbance	Average concentration NO (µg/mL)	St Dev
Control	0,071	0,072	0,072	1,642156863	0,311958874
Control 2	0,07	0,064	0,067		
Control +LPS	0,064	0,064	0,064		
Control 2 +LPS	0,069	0,069	0,069	1,37254902	0,346620971
PDGF-β	0,062	0,062	0,062	0,637254902	0,415945165
PDGF-β 2	0,056	0,056	0,056		
PDGF-β +LPS	0,057	0,055	0,056		
PDGF-β 2 +LPS	0,06	0,059	0,060	0,514705882	0,24263468
IFN-γ	0,07	0,07	0,070	1,764705882	0,069324194
IFN-γ 2	0,078	0,064	0,071		
IFN-γ +LPS	0,232	0,237	0,235	19,53431373	2,391684701

IFN-γ 2 +LPS	0,266	0,272	0,269		

*Table 9: Absorbance and concentration NO assay experiment 2 (**Figure 8**)*

Treatment	Absorbance 1	Absorbance 2	Average absorbance	Average concentration NO (µg/mL)	St Dev
Control	0,062	0,062	0,062	0,525252525	0,116636
Control 2	0,06	0,06	0,06		
IFN-γ +LPS	0,08	0,08	0,08	2,545454545	0,116636
IFN-γ +LPS 2	0,082	0,082	0,082		
IL-10	0,06	0,058	0,059	0,222222222	0,14285
IL-10 2	0,057	0,057	0,057		
IL-10 +LPS	0,056	0,057	0,0565	0,222222222	0,184418
IL-10 LPS 2	0,059	0,06	0,0595		
IFN-γ + IL-10	0,061	0,06	0,0605	0,474747475	0,058318
IFN-γ + IL-10 2	0,061	0,06	0,0605		
IFN-γ + IL-10 +LPS	0,074	0,075	0,0745	1,914141414	0,050505
IFN-γ + IL-10 +LPS 2	0,075	0,075	0,075		

*Table 10: Absorbance and concentration NO assay experiment 3 (**Figure 9**)*

	Treatment	Absorbance 1	Absorbance 2	Average absorbance	Average Concentration NO (µg/mL)	St Dev
-LPS	Control	0,063	0,063			
	Control 2	0,06	0,062		0,8	0,14
	IL-10	0,061	0,059			
	IL-10 2	0,059	0,058		0,6	0,13
	IFN-γ + IL-10	0,064	0,062			
	INF-γ + IL-10 2	0,062	0,063		0,9	0,10
	IFN-γ	0,064	0,064			
	INF-γ 2	0,061	0,061		0,9	0,17
	IFN-γ 3	0,064	0,064			
	INF-γ 3 - 2	0,062	0,064		1,0	0,10
+LPS	Control	0,062	0,062			
	Control 2	0,064	0,065		0,96	0,15
	IL-10	0,058	0,059			
	IL-10 2	0,061	0,061		0,61	0,15
	IL-10 + IFN-γ	0,202	0,203			
	IL-10 + IFN-γ 2	0,204	0,204		15,11	0,10
	IFN-γ	0,186	0,185			
	IFN-γ 2	0,192	0,194		13,69	0,45
	IFN-γ 3	0,068	0,068			
	IFN-γ 3 - 2	0,073	0,072		1,67	0,27

*Table 11: Absorbance and concentration NO assay experiment 4 (**Figure 10**)*

Treatment	Absorbance 1	Absorbance 2	Average absorbance	Average concentration NO (µg/mL)	St Dev
Control	0,071	0,067	0,069	0,7	0,32
Control +LPS	0,064	0,065	0,0645	0,1	0,08

IFN-γ	0,065	0,064	0,0645	0,1	0,08
IFN-γ +LPS	0,179	0,178	0,1785	13,0	0,08
TGF-β	0,063	0,061	0,062	0,0	0,16
TGF-β +LPS	0,06	0,06	0,06	0,0	0,00
IL-10	0,06	0,06	0,06	0,0	0,00
IL-10 +LPS	0,062	0,062	0,062	0,0	0,00

Appendix L: Pictures 3T3 cells NO assay

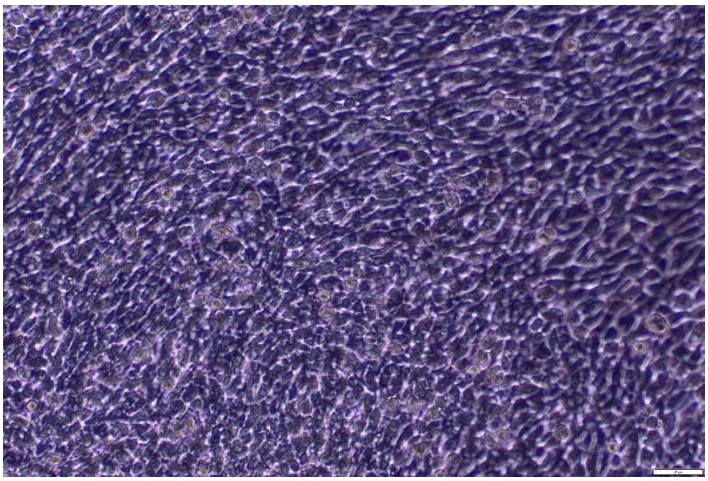

Figure 18: NIH-3T3 cells from experiment 1 after 48h control, stimulated with LPS (100 ng/mL)

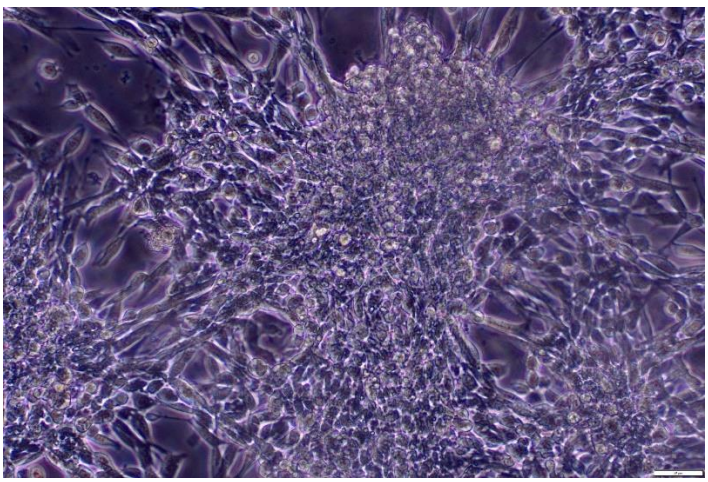

Figure 19: NIH-3T3 cells from experiment 1 after 48h, stimulated with PDGF (40 ng/mL) and LPS (100 ng/mL)

Appendix M: Raw data DHPAA-assay

*Table 12: Table showing the raw data of the standard curve DHPAA-assay that is shown in **Appendix E.***

Collagen concentration (µg/mL)	Absorbance 1	Absorbance 2	Absorbance 3	Average absorbance	St Dev
0	41882	42290	43296	42489,33	727,7701
1	16901	16681	16937	16839,67	138,5833
3	8605	8857	8996	8819,333	198,2028
10	6490	6768	21451	11569,67	8558,615
30	5253	5208	5488	5316,333	150,3607
100	5156	5176	5205	5179	24,63737
300	5263	5125	5057	5148,333	104,9635

*Table 13: Absorbance and concentration DHPAA-assay experiment 1 (**Figure 11**)*

Treatment	Absorbance 1	Absorbance 2	Average absorbance	Average concentration collagen (µg/mL)	St Dev
Control 24h	5803	5544	5673,5	5,2	1,5
Control 48h	6311	6653	6482	11,8	2,0
Control 72h	6084	6223	6153,5	9,1	0,8
TGF-β 24h	6836	6917	6876,5	15,0	0,5
TGF-γ 48h	5689	6057	5873	6,8	2,1
TGF-γ 72h	5734	5753	5743,5	5,8	0,1

*Table 14: Absorbance and concentration DHPAA-assay experiment 2 (**Figure 11**)*

Treatment	Absorbance 1	Absorbance 2	Average absorbance	Average concentration collagen (µg/mL)	St Dev
Control 24h	23604	24454	24029	136	7
Control 48h	31709	21231	26470	163	82
Control 72h	19169	18991	19080	82	1
TGF-β 24h	20872	20239	20555,5	98	5
TGF-γ 48h	25970	21622	23796	134	34
TGF-γ 72h	21335	82530	51932,5	444	477

Appendix N: Raw data protein assay

*Table 15: Table showing the raw data of the standard curve of the protein assay that is shown in **Appendix G.***

BSA Concentration (µg/µL)	Absorbance 1	Absorbance 2	Absorbance 3	Average absorbance	St Dev
10	1,002	1,035	1,039	1,025333	0,020306
8	0,858	0,94	0,91	0,902667	0,041489
6	0,816	0,844	0,84	0,833333	0,015144
4	0,638	0,626	0,647	0,637	0,010536
3	0,532	0,53	0,536	0,532667	0,003055
2	0,405	0,413	0,404	0,407333	0,004933
1	0,275	0,273	0,255	0,267667	0,011015
0,5	0,186	0,19	0,194	0,19	0,004
0,25	0,14	0,143	0,137	0,14	0,003
0,125	0,111	0,112	0,114	0,112333	0,001528
0,06	0,092	0,094	0,092	0,092667	0,001155
0,03	0,089	0,093	0,092	0,091333	0,002082

*Table 16: Absorbance and concentration protein assay experiment 1 of DHPAA-assay (**Figure 12**)*

Treatment	Absorbance 1	Absorbance 2	Average absorbance	Average concentration BSA (µg/µL)	St Dev
Control 24h	0,493	0,425	0,459	2,8	0,428706
Control 48h	0,424	0,451	0,438	2,7	0,165738
Control 72h	0,424	0,463	0,444	2,7	0,24114
TGF-β 24h	0,409	0,443	0,426	2,6	0,205955
TGF-γ 48h	0,385	0,393	0,389	2,2	0,046521

TGF-γ 72h	0,619	0,509	0,564	3,8	0,808892

*Table 17: Absorbance and concentration protein assay experiment 2 of DHPAA-assay (**Figure 12**)*

Treatment	Absorbance 1	Absorbance 2	Average absorbance	Average concentration BSA (µg/µL)	St Dev
Control 24h	0,299	0,302	0,3005	1,30	0,014527
Control 48h	0,376	0,343	0,3595	1,72	0,166883
Control 72h	0,533	0,492	0,5125	2,89	0,237045
TGF-β 24h	0,414	0,419	0,4165	2,13	0,026467
TGF-γ 48h	0,462	0,454	0,458	2,45	0,043907
TGF-γ 72h	0,528	0,526	0,527	3,00	0,011733

Appendix O: Raw data qPCR

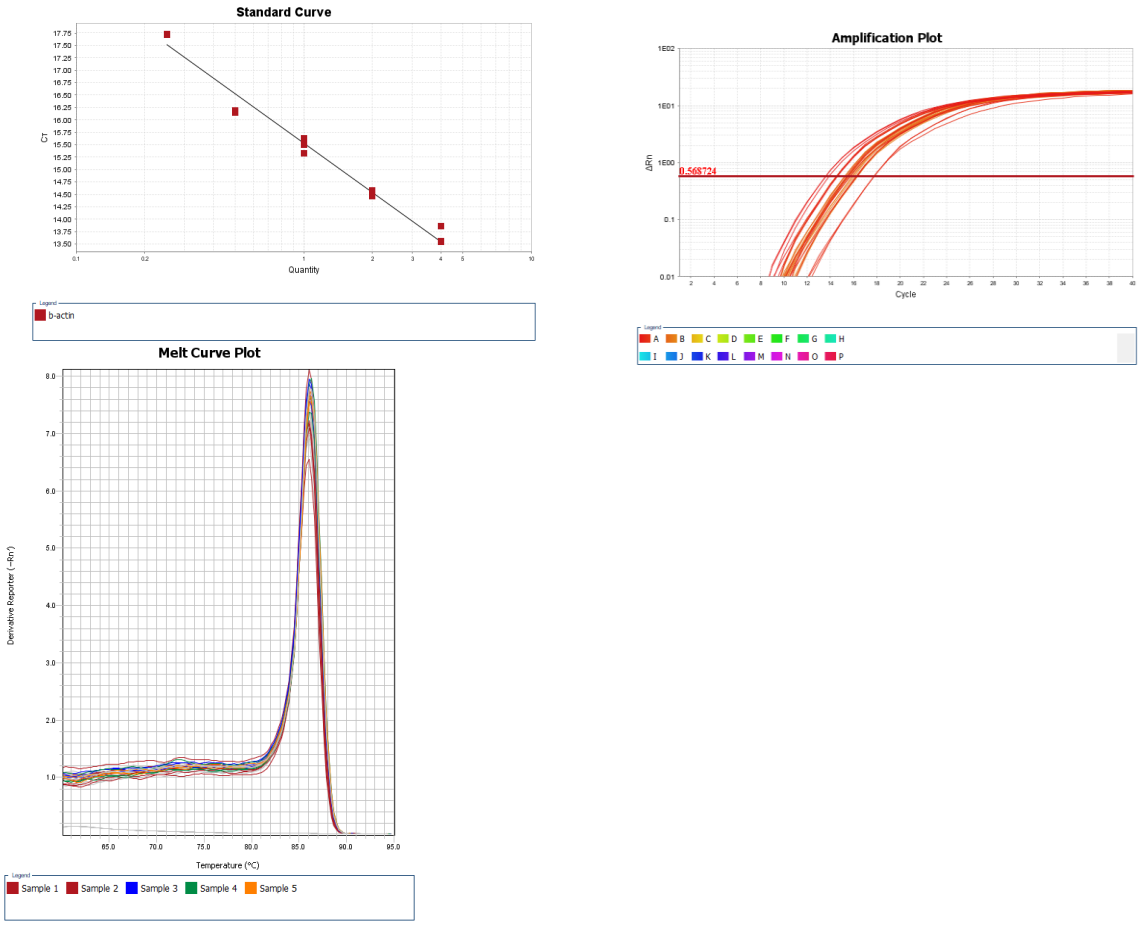

Figure 20: Standard curve, amplification curve and melting curve of β-actin obtained with qPCR.

Table 18: Ct, Quantity and Melting Temperature 1 and 2 of β-actin of the standard curve.

Sample	CT	Quantity	Tm1	Tm2
STD 4	13,859	4,000	85,911	
STD 4	13,562	4,000	86,043	
STD 4	13,549	4,000	86,043	
STD 2	14,587	2,000	86,043	
STD 2	14,499	2,000	86,043	
STD 2	14,460	2,000	86,043	
STD 1	15,328	1,000	86,043	

STD 1	15,634	1,000	86,043	
STD 1	15,498	1,000	86,043	
STD 0.5	16,193	0,500	86,175	
STD 0.5	16,148	0,500	86,175	
STD 0.5	16,774	0,500	86,175	
STD 0.25	17,733	0,250	86,175	
STD 0.25	17,732	0,250	86,043	
STD 0.25	17,709	0,250	86,043	

*Table 19: Ct, quantity, melting temperature 1 and 2, average quantity and standard deviation of β-actin (**Figure 13**)*

Treatment	CT	Quantity	Tm1	Tm2	Average quantity	St Dev
Control	15,637	0,942	86,043		0,974	0,049
Control	15,626	0,949	86,043			
Control	15,507	1,031	86,043			
Control +LPS	15,171	1,302	86,043		1,298	0,025
Control +LPS	15,150	1,321	86,043			
Control +LPS	15,206	1,270	86,043			
TGF-β +LPS	15,470	1,058	86,175		1,095	0,041
TGF-β +LPS	15,429	1,088	86,175			
TGF-β +LPS	15,364	1,139	86,175			
IFN-γ +LPS	15,963	0,751	86,175		0,790	0,035
IFN-γ +LPS	15,836	0,821	86,175			
IFN-γ +LPS	15,876	0,798	86,175			
IFN-γ + IL-10 +LPS	16,239	0,620	86,175		0,634	0,029
IFN-γ + IL-10 +LPS	16,133	0,668	86,175			
IFN-γ + IL-10 +LPS	16,252	0,615	86,175			
Negative control	Undetermined		61,502	85,779		
Negative control	Undetermined		61,238	90,397		
Positive control	14,508	2,061	86,175			
Positive control	14,434	2,171	86,175			

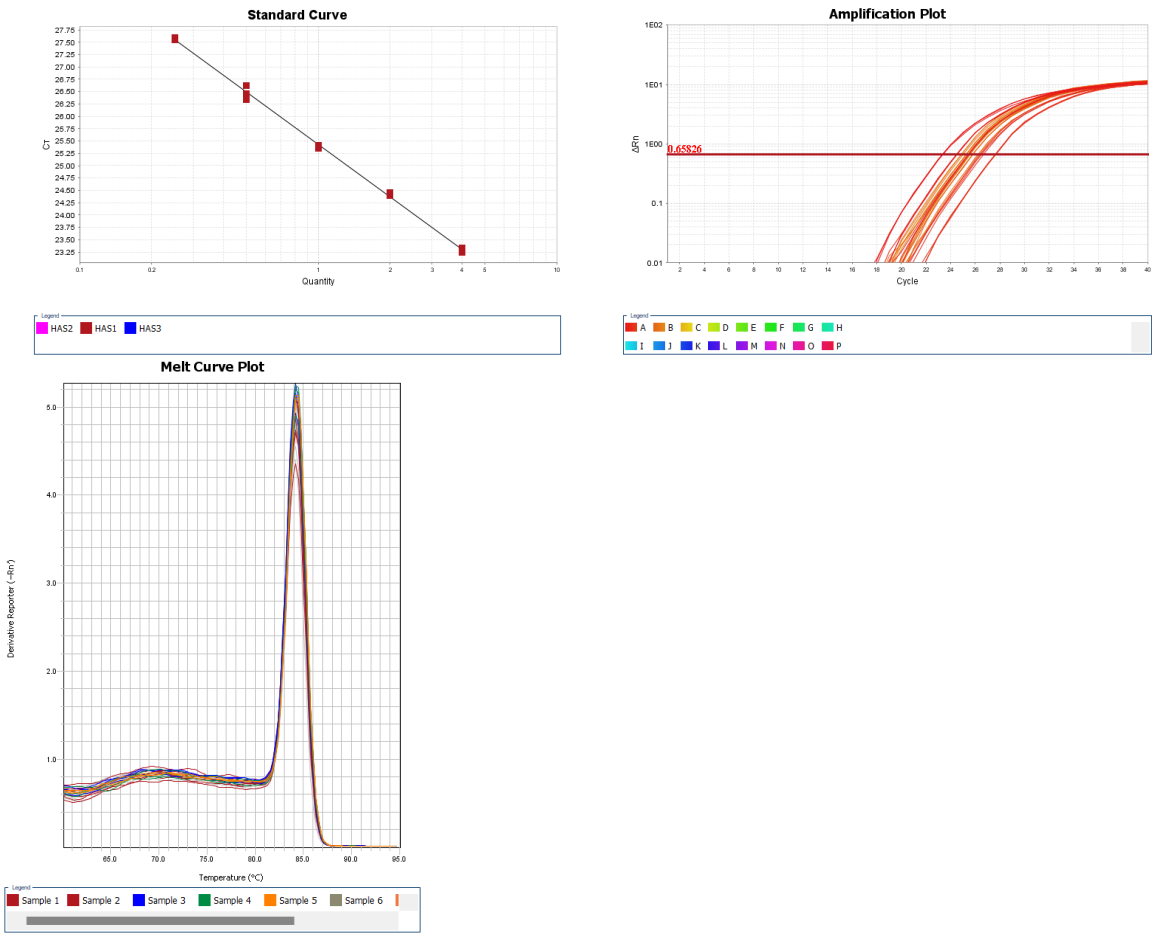

Figure 21: Standard curve, amplification curve and melting curve of HAS1 obtained with qPCR.

Table 20: Ct, Quantity and Melting Temperature 1 and 2 of HAS1 of the standard curve.

Samples	CT	Quantity	Tm1	Tm2
STD 4	23,326	4,000	84,064	
STD 4	23,246	4,000	84,064	
STD 4	23,284	4,000	84,196	
STD 2	24,417	2,000	84,196	
STD 2	24,399	2,000	84,064	
STD 2	24,454	2,000	84,196	
STD 1	25,349	1,000	84,196	
STD 1	25,355	1,000	84,196	
STD 1	25,409	1,000	84,196	
STD 0.5	26,343	0,500	84,196	
STD 0.5	26,464	0,500	84,196	
STD 0.5	26,618	0,500	84,328	
STD 0.25	27,556	0,250	84,328	
STD 0.25	27,599	0,250	84,328	
STD 0.25	27,552	0,250	84,328	

*Table 21: Ct, quantity, melting temperature 1 and 2, average quantity and standard deviation of HAS1 (**Figure 14**)*

Treatment	CT	Quantity	Tm1	Tm2	Average quantity	St dev
Control	26,146	0,624	84,196		0,714954197	0,203509
Control	25,506	0,948	84,196			
Control	26,279	0,573	84,196			

Control +LPS	25,756	0,806	84,196		0,80708915	0,001654
Control +LPS	25,754	0,807	84,196			
Control +LPS	25,750	0,809	84,196			
TGF-β +LPS	25,535	0,930	84,196		0,954909742	0,021297
TGF-β +LPS	25,474	0,968	84,196			
TGF-β +LPS	25,477	0,966	84,196			
IFN-γ +LPS	24,969	1,347	84,328		1,441306829	0,083617
IFN-γ +LPS	24,832	1,473	84,328			
IFN-γ +LPS	24,799	1,505	84,328			
IFN-γ + IL-10 +LPS	25,194	1,162	84,328		1,169863105	0,011517
IFN-γ + IL-10 +LPS	25,167	1,183	84,328			
IFN-γ + IL-10 +LPS	25,191	1,164	84,328			
Negative control	Undetermined		61,369	84,328		
Negative control	Undetermined		61,369	84,064		
Negative control	Undetermined		61,369			
Positive control	26,678	0,441	84,592			
Positive control	26,587	0,468	84,460			

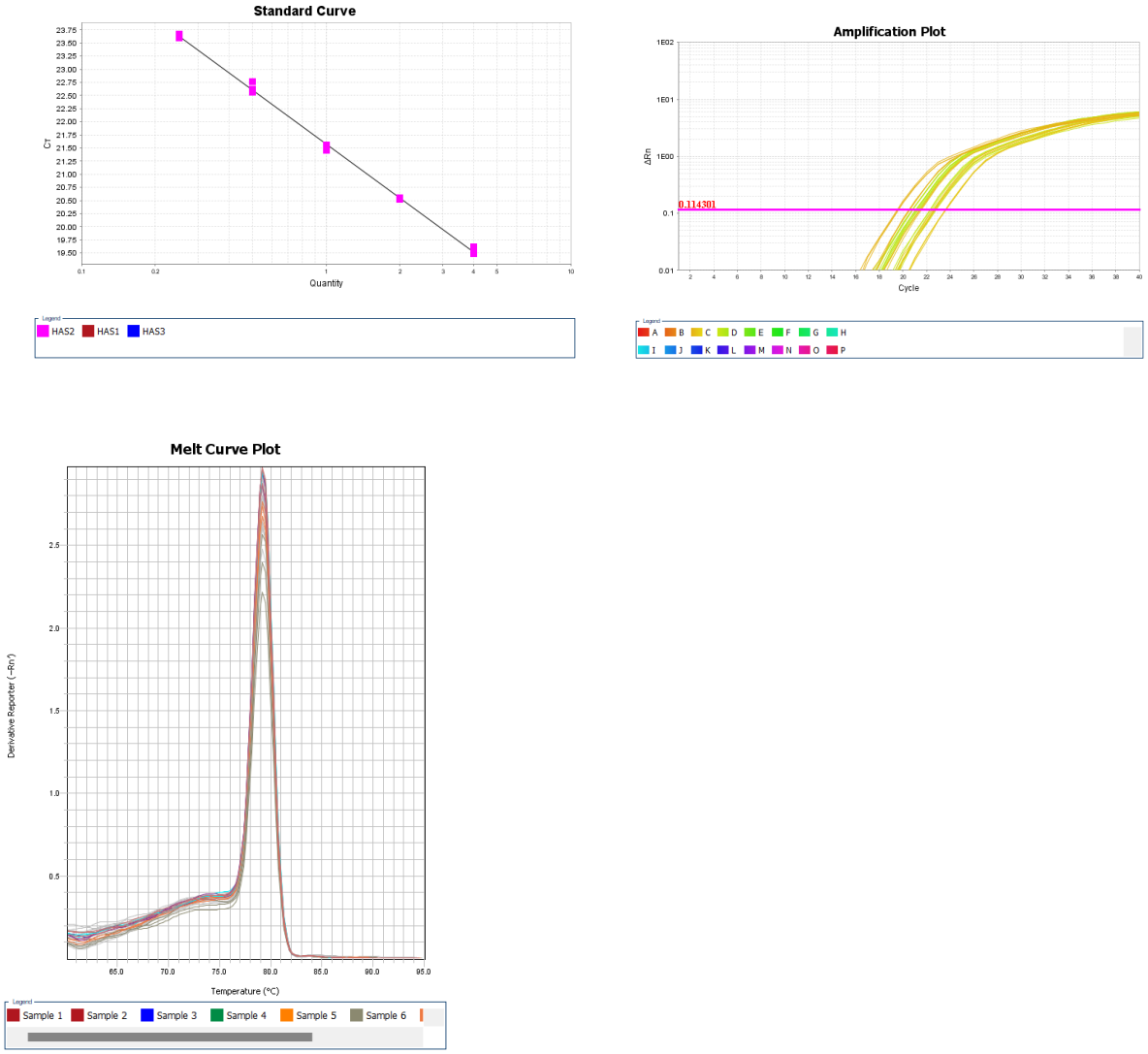

Figure 22: Standard curve, amplification curve and melting curve of HAS2 obtained with qPCR.

Table 22: Ct, Quantity and Melting Temperature 1 and 2 of HAS2 of the standard curve.

Samples	CT	Quantity	Tm1	Tm2
STD 4	19,571	4,000	79,182	
STD 4	19,613	4,000	79,182	
STD 4	19,492	4,000	79,182	
STD 2	20,559	2,000	79,182	
STD 2	20,538	2,000	79,182	
STD 2	20,517	2,000	79,182	
STD 1	21,469	1,000	79,182	
STD 1	21,459	1,000	79,182	
STD 1	21,555	1,000	79,182	
STD 0.5	22,760	0,500	79,182	
STD 0.5	22,560	0,500	79,182	
STD 0.5	22,621	0,500	79,182	
STD 0.25	23,674	0,250	79,182	
STD 0.25	23,601	0,250	79,182	
STD 0.25	23,630	0,250	79,314	

*Table 23: Ct, quantity, melting temperature 1 and 2, average quantity and standard deviation of HAS2 (**Figure 14**)*

Treatment	CT	Quantity	Tm1	Tm2	Average quantity	St Dev
Control	22,802	0,437	79,182		0,454831	0,018583
Control	22,743	0,454	79,182			
Control	22,681	0,474	79,314			
Control +LPS	22,263	0,628	79,182		0,600393	0,036396
Control +LPS	22,435	0,559	79,182			
Control +LPS	22,297	0,614	79,182			
TGF-β +LPS	21,268	1,230	79,182		1,18709	0,045798
TGF-β +LPS	21,382	1,139	79,182			
TGF-β +LPS	21,315	1,192	79,182			
IFN-γ +LPS	20,808	1,679	79,182		1,665413	0,011835
IFN-γ +LPS	20,823	1,662	79,182			
IFN-γ +LPS	20,828	1,656	79,182			
IFN-γ + IL-10 +LPS	21,104	1,374	79,182		1,369131	0,026723
IFN-γ + IL-10 +LPS	21,141	1,340	79,182			
IFN-γ + IL-10 +LPS	21,084	1,393	79,314			
Negative control	31,251		79,446			
Negative control	Undetermined		78,654	61,501		
Negative control	32,756		79,446			

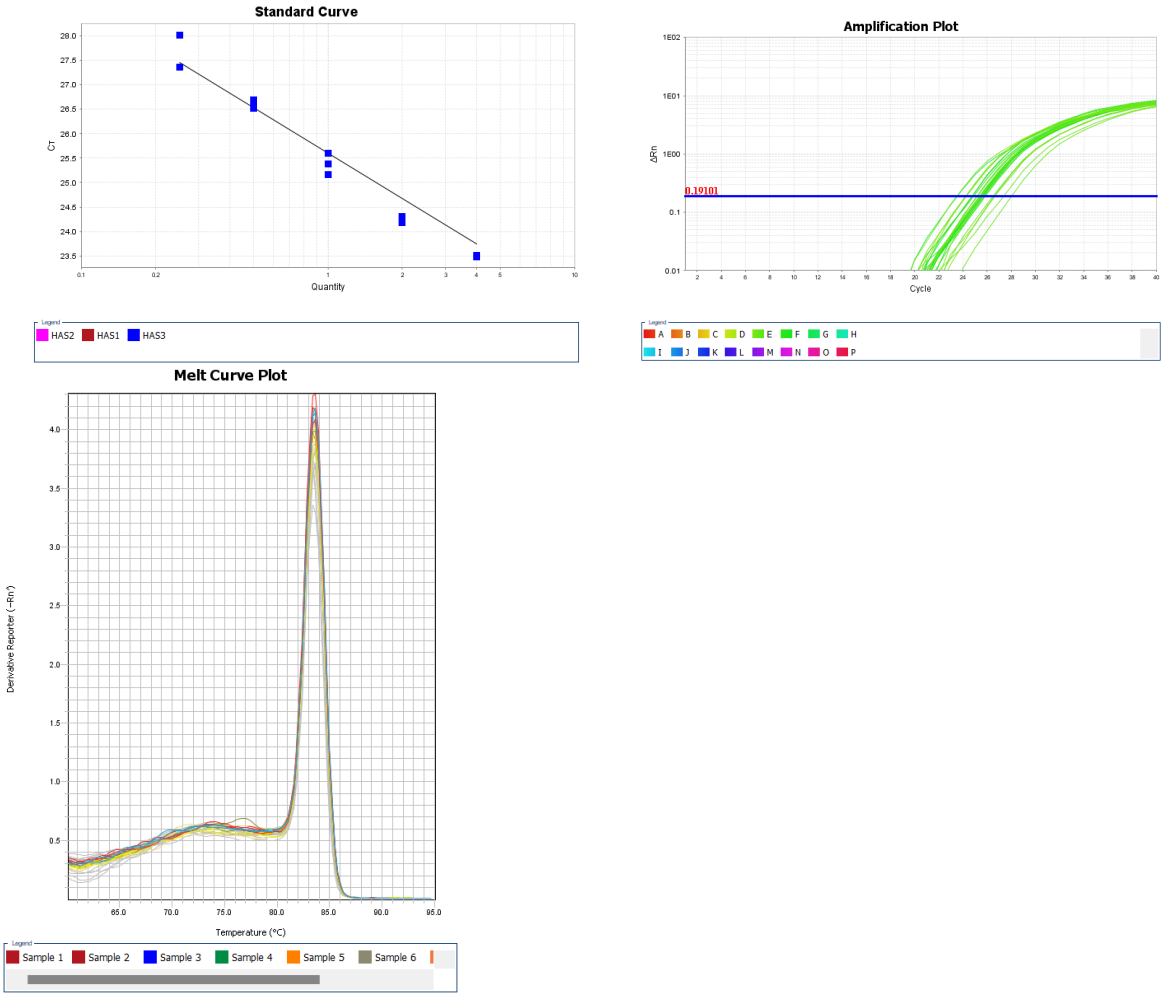

Figure 23: Standard curve, amplification curve and melting curve of HAS3 obtained with qPCR.

Table 24: Ct, Quantity and Melting Temperature 1 and 2 of HAS3 of the standard curve.

Samples	CT	Quantity	Tm1	Tm2
STD 4	25,475	4,000	83,536	
STD 4	23,483	4,000	83,536	
STD 4	Undetermined	4,000	83,668	
STD 4	23,510	4,000	83,668	
STD 2	24,187	2,000	83,272	
STD 2	24,313	2,000	83,536	
STD 2	24,270	2,000	83,404	
STD 1	25,375	1,000	83,536	
STD 1	25,158	1,000	83,536	
STD 1	25,605	1,000	83,536	
STD 0.5	26,623	0,500	83,404	
STD 0.5	26,696	0,500	83,536	
STD 0.5	26,524	0,500	83,536	
STD 0.25	27,361	0,250	83,536	
STD 0.25	Undetermined	0,250	79,182	61,369
STD 0.25	28,020	0,250	83,668	

*Table 25: Ct, quantity, melting temperature 1 and 2, average quantity and standard deviation of HAS3 (**Figure 14**)*

Treatment	CT	Quantity	Tm1	Tm2	Average quantity	St Dev
Control	25,440	1,130	83,536		1,039788	0,07846

Control	25,612	0,993	83,536			
Control	25,610	0,996	83,536			
Control +LPS	25,807	0,859	83,536		0,8833	0,097405
Control +LPS	25,616	0,991	83,536			
Control +LPS	25,901	0,800	83,536			
TGF-β +LPS	25,702	0,929	83,536		0,975197	0,076769
TGF-β +LPS	25,697	0,933	83,536			
TGF-β +LPS	25,521	1,064	83,536			
IFN-γ +LPS	24,749	1,895	83,536		1,81002	0,097925
IFN-γ +LPS	24,794	1,832	83,536			
IFN-γ +LPS	24,892	1,703	83,536			
IFN-γ + IL-10 +LPS	25,449	1,122	83,536		1,166387	0,170531
IFN-γ + IL-10 +LPS	25,574	1,022	83,536			
IFN-γ + IL-10 +LPS	25,198	1,355	83,536			
Negative control	Undetermined		77,862	61,369		
Negative control	Undetermined		61,369			
Negative control	39,459		77,862	61,369		